

WestminsterResearch

<http://www.westminster.ac.uk/westminsterresearch>

Study on the pulmonary delivery system of apigenin loaded albumin nanocarriers with antioxidant activity

Papay, Z.E., Kosa, A., Boddi, B., Merchant, Z., Saleem, I.Y., Zariwala, M., Klebovich, I., Somavarapu, S. and Antal, I.

This is an author's accepted manuscript of an article published in the Journal of Aerosol Medicine and Pulmonary Drug Delivery doi:10.1089/jamp.2016.1316.

The final definitive version is available online at:

<https://dx.doi.org/10.1089/jamp.2016.1316>

The WestminsterResearch online digital archive at the University of Westminster aims to make the research output of the University available to a wider audience. Copyright and Moral Rights remain with the authors and/or copyright owners.

Whilst further distribution of specific materials from within this archive is forbidden, you may freely distribute the URL of WestminsterResearch: (<http://westminsterresearch.wmin.ac.uk/>).

In case of abuse or copyright appearing without permission e-mail repository@westminster.ac.uk

Journal of Aerosol Medicine and Pulmonary Drug Delivery; <http://mc.manuscriptcentral.com/aerosol>

Study on the pulmonary delivery system of apigenin loaded albumin nanocarriers with antioxidant activity

Journal:	<i>Journal of Aerosol Medicine and Pulmonary Drug Delivery</i>
Manuscript ID	JAMP-2016-1316.R2
Manuscript Type:	Original Research
Date Submitted by the Author:	03-Jan-2017
Complete List of Authors:	Papay, Zsofia; Semmelweis University, Department of Pharmaceutics Kosa, Annamaria; Institute of Biology, Eötvös Lóránd University, Department of Plant Anatomy Boddi, Bela; Institute of Biology, Eötvös Lóránd University, Department of Plant Anatomy Merchant, Zahra; University College London School of Pharmacy Saleem, Imran; Liverpool John Moores University, School of Pharmacy & Biomolecular Sciences Zariwala, Mohammed ; University of Westminster Klebovich, Imre; Semmelweis University, Department of Pharmaceutics Somavarapu, Satyanarayana ; University College London School of Pharmacy Antal, Istvan; Semmelweis Egyetem, Department of Pharmaceutics
Keyword:	Aerosol Distribution, inhaled therapy, Modeling
Manuscript Keywords (Search Terms):	flavonoid, apigenin, albumin nanoparticles

SCHOLARONE™
Manuscripts

Study on the pulmonary delivery system of apigenin loaded albumin nanocarriers with antioxidant activity

Zsófia Edit Pápay¹, Annamária Kósa, PhD², Béla Böddi, PhD², Zahra Merchant³, Imran Y Saleem, PhD⁴, Mohammed Gulrez Zariwala, PhD⁵, Imre Klebovich, PhD¹, Satyanarayana Somavarapu, PhD^{3*}, István Antal, PhD^{1*}

¹ Department of Pharmaceutics, Semmelweis University, Hógyes E. Street 7-9, H-1092 Budapest, Hungary

² Department of Plant Anatomy, Institute of Biology, Eötvös Lóránd University, Pázmány Péter Street 1/C, Budapest, Hungary

³ Department of Pharmaceutics, UCL School of Pharmacy, 29-39 Brunswick Square, London WC1N 1AX, United Kingdom

⁴ Formulation and Drug Delivery Research, School of Pharmacy and Biomolecular Sciences, Liverpool John Moores University, Liverpool, United Kingdom

⁵ Department of Biomedical Science, Faculty of Science and Technology, University of Westminster, 115 New Cavendish Street, London, W1W 6UW, United Kingdom

* To whom correspondence should be addressed:

antal.istvan@pharma.semmelweis-univ.hu

Department of Pharmaceutics

Semmelweis University

Hógyes E. Street 7-9,

H-1092 Budapest, Hungary

Tel/Fax: +3612017-0914; Tel.: +361476-3600/53066, 53087

Running title:

Albumin-Apigenin Nanoparticles against Lung Injury

1
2
3 1 **Study on the pulmonary delivery system of apigenin loaded albumin**
4
5 2 **nanocarriers with antioxidant activity**
6

7
8 3 Zsófia Edit Pápay¹, Annamária Kósa, PhD², Béla Böddi, PhD², Zahra Merchant³, Imran Y
9 4 Saleem, PhD⁴, Mohammed Gulrez Zariwala, PhD⁵, Imre Klebovich, PhD¹, Satyanarayana
10 5 Somavarapu, PhD^{3*}, István Antal, PhD^{1*}
11

12
13 6 ¹ Department of Pharmaceutics, Semmelweis University, Hőgyes E. Street 7-9, H-1092
14 7 Budapest, Hungary
15

16
17 8 ² Department of Plant Anatomy, Institute of Biology, Eötvös Lóránd University, Pázmány
18 9 Péter Street 1/C, Budapest, Hungary
19

20
21 10 ³ Department of Pharmaceutics, UCL School of Pharmacy, 29-39 Brunswick Square, London
22 11 WC1N 1AX, United Kingdom
23

24
25 12 ⁴ Formulation and Drug Delivery Research, School of Pharmacy and Biomolecular Sciences,
26 13 Liverpool John Moores University, Liverpool, United Kingdom
27

28
29 14 ⁵ Department of Biomedical Science, Faculty of Science and Technology, University of
30 15 Westminster, 115 New Cavendish Street, London, W1W 6UW, United Kingdom
31

32
33
34 16 * To whom correspondence should be addressed:

35
36 17 antal.istvan@pharma.semmelweis-univ.hu
37

38
39 18 Department of Pharmaceutics

40
41 19 Semmelweis University

42
43 20 Hőgyes E. Street 7-9,

44
45 21 H-1092 Budapest, Hungary

46
47 22 Tel/Fax: +3612017-0914; Tel.: +361476-3600/53066, 53087
48

49
50 23 **Running title:**

51
52 24 **Albumin-Apigenin Nanoparticles against Lung Injury**
53

54
55
56
57
58
59
60

ABSTRACT

26 **Background:** Respiratory diseases are mainly derived from acute and chronic inflammation
27 of the alveoli and bronchi. The pathophysiological mechanisms of pulmonary inflammation
28 mainly arise from oxidative damage that could ultimately lead to acute lung injury (ALI).
29 Apigenin (Api) is a natural polyphenol with prominent antioxidant and anti-inflammatory
30 properties in the lung. Inhalable formulations consist of nanoparticles (NPs) have several
31 advantages over other administration routes therefore this study investigated the application of
32 apigenin loaded bovine serum albumin nanoparticles (BSA-Api-NPs) for pulmonary delivery.

33 **Methods:** Dry powder formulations of BSA-Api-NPs were prepared by spray drying and
34 characterized by laser diffraction particle sizing, scanning electron microscopy, differential
35 scanning calorimetry and powder X-ray diffraction. The influence of dispersibility enhancers
36 (lactose monohydrate and L-leucine) on the *in vitro* aerosol deposition using a next generation
37 impactor (NGI) was investigated in comparison to excipient-free formulation. The dissolution
38 of Api was determined in simulated lung fluid by using Franz cell apparatus. The antioxidant
39 activity was determined by 2,2-Diphenyl-1-picrylhydrazyl (DPPH') free radical scavenging
40 assay.

41 **Results:** The encapsulation efficiency and the drug loading was measured to be $82.61 \pm$
42 4.56% and $7.51 \pm 0.415\%$. The optimized spray drying conditions were suitable to produce
43 particles with low residual moisture content. The spray dried BSA-Api-NPs possessed good
44 the aerodynamic properties due to small and wrinkled particles with low mass median
45 aerodynamic diameter, high emitted dose and fine particle fraction. The aerodynamic
46 properties was enhanced by leucine and decreased by lactose, however, the dissolution was
47 reversely affected. The DPPH' assay confirmed that the antioxidant activity of encapsulated
48 Api was preserved.

1
2
3 49 **Conclusion:** This study provides evidence to support that albumin nanoparticles are suitable
4
5 50 carriers of Api and the use of traditional or novel excipients should be taken into
6
7 51 consideration. The developed BSA-Api-NPs is a novel delivery system against lung injury
8
9
10 52 with potential antioxidant activity.

11
12 53 **Keywords:** aerosol distribution, inhaled therapy, modeling
13
14 54

1. INTRODUCTION

Respiratory diseases are thought to be mainly derived from acute and chronic inflammation of the alveoli and the bronchi. The pathophysiological mechanisms of pulmonary inflammation arise from several factors, including oxidative damage due to cytotoxic mediators that may ultimately lead to acute lung injury (ALI), acute respiratory distress syndrome (ARDS) and cancer¹. A growing body of scientific data suggests that natural occurring compounds possess preventive and therapeutic properties with inherent low toxicity². Among phytochemicals, apigenin (Api, **Figure 1**) is a promising candidate as a therapeutic agent, mainly due to its antioxidant and anti-inflammatory properties³⁻⁶. It has been demonstrated that Api has protective effects against bleomycin-induced lung fibrosis in rats which is associated with its antioxidant and anti-inflammatory capacities⁷. Another study provided evidence that Api has been able to decrease oxidative stress and inflammation on paraquat-induced ALI in mice⁸ and reduced the pathological alterations of pulmonary tissue in acute pancreatitis associated ALI, therefore suggesting protection in the lung⁹. Furthermore, Api has anti-inflammatory effect owing to significant inhibition of pro-inflammatory cytokines, activator protein (AP-1) and cyclooxygenase-2 (COX-2) in human pulmonary epithelial cells¹⁰ and in mice as well¹¹. However, Api's has low water solubility (2.16 µg/ml at pH 7.5) and therefore it was recently classified as BCS (Biopharmaceutical Classification System) II. drug¹².

Encapsulation and delivery of phytoconstituents with health effects has attracted much attention in recent years. Developing a suitable carrier system is essential to improve the overall activity and reduce the possible toxicity of these agents¹³. Among the potential carrier systems, serum albumin nanoparticles have notable advantages including biodegradability, non-antigenicity and cell-targeting ability^{14,15}. Moreover, albumin provide exceptional ligand binding capacity for various drugs owing to three homologous domains with two separate

1
2
3 80 helical subdomains¹⁶. Studies reported the successful incorporation of flavonoids into albumin
4
5 81 nanoparticles that can improve their stability¹⁷ and antitumor activity¹⁸.

6
7 82 Pulmonary delivery of pharmacologically active ingredients are extensively studied due to
8
9 83 prominent advantages over other delivery routes of administration¹⁹. The lungs have a large
10
11 84 surface area, limited enzymatic activity and high permeability therefore drugs can be
12
13 85 delivered either locally for the treatment of respiratory diseases or systematically in order to
14
15 86 e.g. avoid first pass metabolism²⁰. Dry Powder Inhaler (DPI) products offer precise and
16
17 87 reproducible delivery of fine drug particle fraction to the deep lung and recent studies have
18
19 88 proved that these are more cost effective than other products²¹. This non-invasive delivery
20
21 89 route could be suitable for poorly water soluble drugs in nanoparticles with increased
22
23 90 solubility²². It is also well recognized that nanoparticles have benefits over other carriers in
24
25 91 the micron scale such as controlled drug release, avoiding mucociliary clearance and improve
26
27 92 deposition^{23, 24}. Albumin is naturally present in the body, as well as in the lung epithelium²⁴,
28
29 93 moreover, the body can absorb proteins into the bloodstream by transcytosis which occurs
30
31 94 deep in the lung and allows drug molecules to pass through cell membrane²⁵. Therefore the
32
33 95 presence of BSA in the nanoparticle system increases membrane permeability, may facilitate
34
35 96 epithelial cell uptake and translocation through the alveo-capillary barrier of the lung²⁶. It
36
37 97 was proved that albumin nanoparticles have high biocompatibility in a wide dose range and
38
39 98 remained longer in the lungs with low systemic exposure²⁴. Thus encapsulation of apigenin
40
41 99 into albumin nanoparticles would enhance its solubility and distribution in the lung. However,
42
43 100 the formulation of dry powders with optimal aerodynamic properties for pulmonary drug
44
45 101 delivery is challenging. Spray drying is a technique for manufacturing respirable dry powders
46
47 102 in one step. During the process, the liquid phase is atomized into droplets that dry rapidly in
48
49 103 the drying chamber due to the compressed air. The process conditions like heat, flow rate,
50
51 104 aspiration rate and pump rate also determine the quality of the product. The thermal
52
53
54
55
56
57
58
59
60

1
2
3 105 degradation caused by overheating can be avoided by the rapid evaporation of the solvent²⁷.
4
5 106 Hence, it is suitable for drying colloidal systems resulting in uniform particle morphology.
6
7 107 Nanoparticle delivery systems targeted to the lungs offer several advantages such as sustained
8
9 108 release, increased local drug concentration and targeted site of action²⁸. Moreover, improved
10
11 109 drug solubility, uniform dose distribution and fewer side effects can be achieved, compared to
12
13 110 conventional dry powders. In general, respirable nanoparticles are embedded in microparticles
14
15 111 in aerodynamic size range²⁶.

16
17
18 112 The aim of this work was to develop a novel dry powder formulation against ALI
19
20 113 caused by oxidative stress. The prepared albumin nanoparticles were characterized in terms of
21
22 114 size, zeta potential and drug loading, additionally the fluorescence properties were
23
24 115 investigated. Following this, the nanoparticles were spray dried with two types of excipients,
25
26 116 namely a traditional lactose monohydrate and a novel amino acid, L-leucine. *In vitro* aerosol
27
28 117 deposition patterns were determined in comparison to excipient-free formulation using a next
29
30 118 generation impactor (NGI) and dissolution test was performed in simulated lung fluid by
31
32 119 using Franz cell apparatus. Laser diffraction particle sizing, morphology and residual moisture
33
34 120 content were measured along with the antioxidant activity.

35 36 37 38 121 **2. MATERIALS AND METHODS**

39 40 122 **MATERIALS**

41
42
43 123 Apigenin (Api) was purchased from (purity > 99%) Hangzhou Dadyangchem Co., Ltd.
44
45 124 (China). Bovine serum albumin powder (BSA, purity \geq 98%), L-leucine, analytical grade
46
47 125 chloroform, acetonitrile and trifluoroacetic acid (TFA) were obtained from Sigma Aldrich
48
49 126 Ltd. (Dorset, UK). Lactohale[®] LH 230 was supplied by Friesland Foods Domo (Amersfoort,
50
51 127 The Netherlands). 2,2-Diphenyl-1-picrylhydrazyl (DPPH[·]) free radical was purchased from
52
53 128 Sigma-Aldrich (Darmstadt, Germany). For the solubility and drug release study, PBS buffer
54
55 129 was purchased (Sigma Aldrich Ltd., Dorset, UK) and simulated lung fluid modified with
56
57
58
59
60

1
2
3 130 0.02% (w/v) (mSLF) was prepared. All of the materials for the mSLF were purchased from
4
5 131 Sigma Aldrich Ltd. (Dorset, UK).
6
7

8 132 **METHODS**

9 133 **2.1. Preparation of BSA-NPs**

10
11
12 134 BSA nanoparticles were prepared using a nanoparticle albumin bound technology with
13
14 135 minor modifications²⁹. Briefly, 1000 mg of BSA was dissolved in 50 ml of distilled water
15
16 136 saturated with chloroform. Separately, 100 mg of Api was dissolved in 3 ml of chloroform
17
18 137 saturated with water and ultrasonicated for 10 minutes. These two solutions were mixed and
19
20 138 ultrasonicated for 20 minutes with a probe-type sonicator (MSE Soniprep 150 Ultrasonic
21
22 139 Processor, MSE Ltd., London, UK) on ice. After homogenization, the chloroform was
23
24 140 evaporated by rotary evaporator (Rotavapor[®] R-10, BÜCHI Labortechnik AG, Flawil,
25
26 141 Switzerland) at 25°C for 15 minutes. The obtained nanoparticles were filtered through filter
27
28 142 paper (0.45µm, Ficher Scientific Ltd., Loughborough, UK) and further spray dried.
29
30
31

32 143 **2.2. Characterization of BSA-Api-NPs**

33 144 **2.2.1. Particle size and zeta potential analysis**

34
35
36 145 The average particle size and polydispersity index (PDI) were determined by dynamic
37
38 146 light scattering (DLS) using Zetasizer Nano ZS instrument (Malvern Instruments Ltd.,
39
40 147 Worcestershire, UK). Zeta potential of the particles was quantified with laser doppler
41
42 148 velocimetry (LDV) using the same instrument. All measurements were performed in triplicate
43
44 149 (n=3) at 25 °C and presented as mean ± standard deviation (SD).
45
46
47

48 150 **2.2.2. Determination of drug loading and encapsulation efficiency**

49
50 151 To determine the amount of Api, 1 ml sample from the BSA-Api formulation was
51
52 152 withdrawn and the apigenin content was determined in mg/ml by adding 5 ml of **dimethyl**
53
54 153 **sulfoxide and methanol (DMSO:MeOH, 50:50% v/v)** and sonicated for 10 minutes. The exact
55
56 154 concentrations were determined after filtration (0.22 µm) by HPLC 1260 (Agilent
57
58
59
60

1
2
3 155 Technologies Inc., Santa Clara, USA) using reverse-phase C₁₈ column (Phenomenex[®],
4
5 156 250x4.6 mm, 4μm) as the stationary phase. The temperature was set to 25 °C. The mobile
6
7 157 phase consisted of 40% acetonitrile and 60% water containing 0.1% (v/v) TFA. The system
8
9 158 was run isocratically at the flow rate of 1.2 ml/min and the Api was detected at 340 nm (t_R =
10
11 159 8.3). The injection volume was set to 10 μl. A calibration curve was conducted by diluting
12
13 160 stock solution (0.1 mg/ml) with R² value of 0.999.

14
15
16 161 The drug loading efficiency (DL, %) and encapsulation efficiency (EE, %) were
17
18 162 calculated according to the equations (Eq. 1. and 2.), comparing the encapsulated Api content
19
20 163 (mg/ml, W_{encapsulated}) to total nanoparticle system which means the weighted amount of BSA
21
22 164 and Api together (mg/ml, W_{total}) and the amount of Api (mg/ml, W_{theoretical}) used in the
23
24 165 formulations.

25
26
27
28 166
$$DL (\%) = \frac{W_{encapsulated}}{W_{total}} \times 100 \quad \text{Eq.1.}$$

29
30
31 167
$$EE (\%) = \frac{W_{encapsulated}}{W_{theoretical}} \times 100 \quad \text{Eq.2.}$$

32 33 168 **2.2.3. Fluorescence spectroscopy**

34
35 169 The fluorescence emission spectra of BSA and BSA-Api-NPs were measured with
36
37 170 Jobin Yvon-Horiba Fluoromax-3 (Paris, France) spectrofluorometer. The samples which
38
39 171 contained the nanoparticles were diluted 10 times and the fluorescence emission spectra were
40
41 172 recorded between 300 and 450 nm at 25 °C where the excitation wavelength was set to 285
42
43 173 nm. The data collection frequency was 0.5 nm and the integration time was 0.2 s. The
44
45 174 excitation slit was set at a bandpass width of 2 nm and the emission slit at 5 nm. Each
46
47 175 spectrum was recorded three times and the mean values were calculated automatically. The
48
49 176 SPSERV V3.14 software (© Csaba Bagyinka, Institute of Biophysics, Biological Research
50
51 177 Center of the Hungarian Academy of Sciences, Szeged, Hungary) was used for baseline
52
53 178 correction, for five point linear smoothing and for the correction to the wavelength-dependent
54
55
56
57
58
59
60

179 sensitivity changes of the spectrofluorometer. The subtraction of the Raman band at 390 nm
180 was performed.

181 To obtain the three-dimensional projections and contour maps of fluorescence spectra
182 of the samples, the fluorescence emission were recorded from 265 to 450 nm using different
183 excitation wavelengths from 250 to 310 nm with 10 nm-steps with the same instrument
184 mentioned above. All emission scan ranges were set to start at least 15 nm away from the
185 corresponding excitation wavelengths. Other settings were similar as described above. Each
186 spectrum was recorded three times and the mean values were calculated automatically. The
187 three-dimensional fluorescence spectra were visualized with the software SURFER Version
188 10 (Golden Software, Inc., Colorado, USA). Spectra were combined together into a three
189 dimensional surface data set with axes of excitation and emission wavelengths and
190 fluorescence intensity. Data were also converted into two dimensional contour maps.

191 **2.3. Spray drying of BSA-Api-NPs**

192 Spray drying of the BSA-Api formulations without excipient and in the presence of
193 lactose monohydrate (50%, w/w) and L-leucine (9%, w/w) were carried out in a Büchi 290
194 Mini Spray Dryer (BÜCHI Labortechnik AG, Flawil, Switzerland). The concentration of the
195 excipients were with respect to the mass of the nanoparticles before spray drying. The
196 following operating conditions were used based on pilot experiments: inlet temperature 120
197 °C, approximate outlet temperature 65-70 °C, the drying airflow 600 L/h, aspiration rate
198 100% (35 m³/h), the nozzle diameter was a 0.1 mm and the liquid feed rate was set to 5
199 ml/min. Each preparation were carried out in triplicate. Following spray drying, the powders
200 were collected from the lower part of the cyclone and the collecting vessel, stored in tightly
201 sealed glass vials under vacuum at room temperature.

202 **2.4. Characterization of spray-dried BSA-Api-NPs**

203 **2.4.1. Determination of residual moisture**

1
2
3 204 The moisture content of the spray-dried powders was measured by using Karl Fischer
4
5 205 titration (Metrohm 758 KFD Titirino, Metrohm AG, Lichtenstein, Switzerland). For that
6
7 206 purpose approx. 100 mg of the product was analysed and the instrument was previously
8
9
10 207 calibrated with 10 μ l distilled water. The evaluation was conducted in triplicate and the
11
12 208 standard deviation calculated.

14 209 **2.4.2. Fourier-Transform Infrared Spectroscopy (FT-IR)**

16 210 FT-IR spectra of BSA-API spray-dried samples were evaluated using a PerkinElmer
17
18 211 Spectrum 100 FT-IR spectrometer equipped with Universal ATR (Attenuated Total
19
20 212 Reflectance) accessory (PerkinElmer Inc., Waltham, USA). Approximately 2 mg of the solid
21
22 213 samples were placed between the plate and the probe. The spectra were recorded with 3 scans,
23
24 214 in the frequency range between 4000-600 cm^{-1} and with a resolution of 4 cm^{-1} at room
25
26 215 temperature. The data were analyzed using the PerkinElmer Spectrum Express software.

29 216 **2.4.3. X-ray powder diffraction (XRPD)**

31 217 XRPD diffractograms were obtained using an X-ray diffractometer (MiniFlex600
32
33 218 Rigaku Corporation, Tokyo, Japan). The analyses were performed at room temperature and
34
35 219 the samples were scanned from 2° to 40° 2 θ using a scanning speed of 2°/min with a step size
36
37 220 of 0.05°.

40 221 **2.4.4. Differential scanning calorimetry (DSC) analysis**

42 222 The spray-dried formulations were characterized by DSC (DSC Q2000 module; TA
43
44 223 Instruments, New Castle, UK) which was calibrated using indium. Samples (3-5 mg) were
45
46 224 weighed accurately and analyzed in sealed and pierced aluminium hermetic pans (TA
47
48 225 Instruments). The pans were equilibrated at 25 °C and then heated at a rate of 10 °C/min in a
49
50 226 range of 50–400 °C.

54 227 **2.4.5. Aerosol particle size analysis and redispersibility in water**

1
2
3 228 The particle size analysis was conducted by using a Sympatec HELOS laser
4
5 229 diffractometer (Sympatec GmbH System-Partikel-Technik, Clausthal-Zellerfeld, Germany).

6
7 230 The powders were dispersed by compressed air (4-5 bar) into the measuring zone of the laser
8
9 231 beam. The optical lens (0.45–87.5 μm size range) focused onto the detector to collect the
10
11 232 diffracted light for calculation of size distribution. The values of 10th (D_{10}), 50th (D_{50}) and
12
13 233 90th (D_{90}) of the cumulative particle size distribution are generated. Samples were measured
14
15 234 in triplicate.

16
17
18 235 The particle size was also determined after spray drying. 5 mg dry powder of each
19
20 236 formulation could be easily redispersed in 5 ml distilled water and the particle size was
21
22 237 determined without any further dilution by the above mentioned Zetasizer Nano ZS
23
24 238 instrument (Malvern Instruments Ltd., Worcestershire, UK).

25 26 27 239 **2.4.6. Solubility and Drug release studies of BSA-Api formulations**

28
29 240 The solubility of BSA-Api formulations were determined in PBS buffer (pH 7.4) and
30
31 241 in modified simulated lung fluid (mSLF, pH 7.4) which contained 0.02% (w/v) DPPC was
32
33 242 prepared according to Son and McConville³⁰. 50 mg of samples of spray dried powders were
34
35 243 added to 100 mL solvent and shaken (150 rpm) for 2 h at 37 °C. At predetermined time points
36
37 244 1 mL of samples were taken from each dissolution media and replaced with the same volume
38
39 245 of fresh medium. All of the samples were diluted with 1 ml methanol and filtered with
40
41 246 Amicon[®] Ultra Centrifugal filters (30K, Merck Millipore, Merck KGaA, Germany) prior to
42
43 247 the injection and the amount of apigenin was determined by HPLC-UV method.

44
45
46 248 The *in vitro* drug release study of the three formulations were conducted with Franz cell
47
48 249 apparatus. The mSLF was used as dissolution media and 0.45 μm cellulose acetate membrane
49
50 250 filter (Sartorius AG, Goettingen, Germany) was applied. Briefly, an accurately weighed
51
52 251 amount (10 mg) of spray dried nanoparticles of each formulations were scattered onto the
53
54 252 membrane which was previously wetted with the dissolution media for 1 hour. 1 ml of
55
56
57
58
59
60

1
2
3 253 samples were withdrawn at various time intervals for 5 hours and replaced with fresh
4
5 254 dissolution medium. After the measurement, membrane was rinsed with 2 ml of MeOH and
6
7 255 the drug content of the possibly remained powders was determined. The sample preparation
8
9
10 256 and the measurement was the same as mentioned above. The cumulative amount of apigenin
11
12 257 release over the time was plotted for each formulations. All measurements were performed in
13
14 258 triplicate.

16 259 **2.4.7. Aerosol delivery of BSA-API formulations**

18
19 260 *In vitro* aerodynamic performance of BSA-API formulations was assessed using the
20
21 261 next generation impactor (NGI; Copley Scientific Ltd., Nottingham, UK), connected
22
23 262 sequentially to a low capacity pump via the critical flow controller (Model LCP5; Copley
24
25 263 Scientific Ltd., Nottingham, UK). During the measurement the pump was operated at air flow
26
27 264 rate of 60 L/min for 4 s. The 3x10 mg powder aliquots from each formulation were loaded
28
29 265 manually into gelatine capsules (size 3) and placed into the inhaler device (Cyclohaler[®],
30
31 266 Pharmachemie, London, UK) which was connected to the NGI via an airtight rubber adaptor
32
33 267 and a stainless steel USP throat. The NGI stages were assembled with an induction port, a
34
35 268 pre-separator and a filter was placed in the final stage. Prior to the impaction, the collection
36
37 269 plates were uniformly coated with 1 ml of 1% silicone oil in N-hexane solution and allowed
38
39 270 to dry leaving a thin film of silicone oil on the plate surface in order to prevent the re-
40
41 271 entrainment of the particles and the pre-separator was filled with 15 ml DMSO:MeOH
42
43 272 (50:50%, v/v) mixture. After the deposition of the powders in the NGI, the amount of each
44
45 273 formulation was cumulatively collected onto silicone-coated plates for each of the stages. The
46
47 274 inhaler, mouth piece, induction port, pre-separator and the collection plates were rinsed with
48
49 275 DMSO:MeOH (50:50%, v/v) mixture, collected in volumetric flasks (10 or 25 ml) and made
50
51 276 up to volume. The samples were determined by using HPLC method as described previously.
52
53
54 277 To characterize the aerosol performance the following parameters were calculated based on
55
56
57
58
59
60

1
2
3 278 the drug mass of each fraction: emitted dose (ED, %): the percentage of the entire dose
4
5 279 depositing from the mouthpiece of the inhaler device and recovered dose (RD, %): the total
6
7 280 recovered drug mass. The fine particle fraction (FPF, $<4.46 \mu\text{m}$) is defined as the percentage
8
9
10 281 of the emitted dose which deposited from the Stage 2-7 and the micro orifice-collector
11
12 282 (MOC). The mass median aerodynamic diameter (MMAD) and geometric standard deviation
13
14 283 (GSD) were calculated from the inverse of the standard normal cumulative mass distribution
15
16 284 against the natural logarithm of the effective cut-off diameter of the respective stages. All
17
18 285 measurements were carried out in triplicate.

20 286 **2.4.8. Particle morphology**

21
22
23 287 Morphology of Api powder and spray-dried nanoparticles was examined using
24
25 288 scanning electron microscopy (SEM) analysis. The dry powder of the formulations was
26
27 289 placed on the sample holder using double adhesive tape and gold coating ($\sim 20 \text{ nm}$ thickness)
28
29 290 was applied. Examinations were performed by FEI InspectTM S50 (Hillsboro, Oregon, USA)
30
31 291 scanning electron microscope at 20.00 kV accelerating voltage. Original magnifications were
32
33 292 8000x, 10,000x and 20,000 x with accuracy of $\pm 2\%$.

34 293 **2.5. Antioxidant activity**

35
36
37 294 The antioxidant activities of the prepared spray-dried formulations were compared to
38
39 295 the pure Api in order to investigate the effectiveness of the formulation. The free radical
40
41 296 scavenging activity was measured by using DPPH[•] method as described previously³¹ with
42
43 297 slight modifications. Methanolic stock solution of 0.1 mM DPPH[•] reagent was freshly
44
45 298 prepared and protected from light. Standard curve was plotted between the DPPH[•]
46
47 299 concentration (0.01-0.1 mM) and absorbance, the linear relationship was calculated
48
49 300 graphically. 1 ml of MeOH was added to the BSA-Api-NPs and the concentration of Api were
50
51 301 the same in each sample for the comparability. Thereafter 2 ml of 0.06 mM DPPH[•] reagent
52
53 302 was added to the samples, vortex mixed for 10 seconds and protected from light. The
54
55
56
57
58
59
60

absorbance at 517 nm was determined with spectrophotometer (UV-Vis spectrophotometer, Metertech SP-8001, Metertech Inc., Taipei, Taiwan) in every 15 minutes until the steady state (when no further discoloration could be observed). The addition of samples resulted decrease in the absorbance of DPPH[•] due to the scavenging activity of Api. The exact concentration of the free radical was calculated using the standard curve. To calculate the inhibition of the free radical DPPH[•] the following equation (Eq.3.) was used:

$$I (\%) = \frac{A_0 - A_s}{A_0} \times 100 \quad \text{Eq.3.}$$

Where I (%) is the inhibition in percent, A_0 is the absorbance of the DPPH[•] solution and A_s is the absorbance of the sample. All measurements were carried out triplicate and the data were expressed as the mean value \pm SD.

3. RESULTS AND DISCUSSION

3.1. Characterization of BSA-Api-NPs

3.1.1. Size, zeta potential and drug content

Albumin is a natural protein that has been widely used as a macromolecular carrier for many drugs with low water solubility. Several techniques are available to prepare albumin nanoparticles including desolvation (coacervation), nab (nanoparticle albumin bound)-technology and self-assembly¹⁴. In this study the BSA-Api-NPs were prepared by using modified nab-technology with ultrasonication. The achieved mean particle size of three samples was 376 ± 7.824 nm with a polydispersity index of 0.285 ± 0.01 . The size of albumin NPs less than 500 nm could localize effectively in the lung. The PDI value indicated narrow particle size distribution and the uniformity of the nanoparticles. The zeta potential was -19.20 ± 0.818 mV. The higher the zeta potential, the more stable the formulation is, less aggregation occurs³². The EE was determined to be $82.61 \pm 4.56\%$ and the DL was $7.51 \pm 0.415\%$. Therefore these results confirmed the high encapsulation efficiency of apigenin by BSA-NPs and it can be attractive tool in encapsulation flavonoids for delivery. Similar data were found

1
2
3 328 in the literature when encapsulating flavonoids into albumin nanoparticles. Human serum
4
5 329 albumin-bound curcumin nanoparticles resulted $7.2 \pm 2.5\%$ loading efficiency³³ and
6
7 330 scutellarin-loaded bovine serum albumin nanoparticles possess 64.46% EE and 6.73% DL³⁴.
8

9 10 331 **3.1.2. Fluorescence spectroscopy**

11 332 The phenomenon of fluorescence quenching can result from various inter and
12
13 333 intramolecular interactions such as energy transfer, conformational changes, complex
14
15 334 formation (static quenching) or collisional interaction (dynamic quenching). During static
16
17 335 quenching the quencher forms a stable non-fluorescent complex with the fluorophore,
18
19 336 however, during dynamic quenching it collides with the fluorophore and facilitates non-
20
21 337 radiative transitions to the ground state³⁵. Therefore quenching of the intrinsic fluorescence of
22
23 338 the two tryptophan residues (Trp-134 and Trp-212) of BSA can offer information about the
24
25 339 changes in molecular microenvironment of these fluorophores, located in domain I and II,
26
27 340 respectively. Trp-134 residue is located close to the protein surface in a hydrophilic
28
29 341 environment, while Trp-212 is within a protein pocket which is hydrophobic (subdomain II
30
31 342 A). The Trp-214 in human serum albumin (HSA) is located similarly to Trp-212 in BSA³⁶⁻³⁸.
32
33 343 The quenching effect of Api on fluorescence intensity of serum albumins (BSA and HSA) has
34
35 344 been studied previously^{36, 39-42} but there is no data related to its behavior in a nanoparticulate
36
37 345 system. Studies have shown that the increasing concentration of Api resulted in a decrease in
38
39 346 the fluorescence emission intensity of serum albumin solutions. This was mainly attributed to
40
41 347 complex formation (static quenching), however, it could be dynamic quenching at higher Api
42
43 348 concentrations⁴². Nevertheless, all studies concluded that Api most likely binds to the sub-
44
45 349 domain IIA of Site I side with electrostatic and hydrophobic interactions, through which H-
46
47 350 bonds and non-radiative energy transfer can occur. The binding could affect the conformation
48
49 351 of Trp micro-region but the secondary structure of serum albumin is not altered^{36, 39, 41}.
50
51
52
53
54
55
56
57
58
59
60

1
2
3 352 However, the pH and ionic concentrations (e.g. NaCl) can affect the fluorescence quenching
4
5 353 on the binding parameters of apigenin to BSA⁴³.
6

7 354 **Figure 2** demonstrates the fluorescence emission spectra of BSA solution, BSA-NPs
8
9 355 and BSA-Api-NPs. The fluorescence intensity of BSA-NPs decreased slightly compared to
10
11 356 BSA solution with no obvious shift of the maximum position at 350 nm. It was probably due
12
13 357 to the conformational changes of the protein. The significantly lower emission intensity of
14
15 358 BSA-Api-NPs indicates that Api could quench the fluorescence of BSA which is also
16
17 359 reflected on the 3D projections (**Figure 3**). All of these findings indicate that Api binds to the
18
19 360 Trp region (Trp-212, subdomain II A) but the spectral maximum was not affected therefore
20
21 361 hydrophobicity and polarity of the fluorophore residues are not altered. It was concluded that
22
23 362 Api can be bound to the Trp region of serum albumin nanoparticles similarly to the solutions.
24
25
26

27 363 **3.2. Characterization of spray-dried BSA-Api-NPs**

28 364 **3.2.1. Determination of residual moisture**

29
30
31 365 Moisture content is mainly influenced by the spray drying conditions. Increased heat
32
33 366 energy availability provided by regulating inlet air temperature and aspirator capacity allows
34
35 367 more efficient drying, thus resulting in the lower moisture content demonstrated. However,
36
37 368 degradation of heat sensitive materials such as proteins may occur; therefore inlet air
38
39 369 temperature should be kept below 120 °C⁴⁴. The water content is also affected by the type of
40
41 370 excipients and the ratio with the nanoparticles⁴⁵. Moisture content is an important factor that
42
43 371 can significantly influence the aerodynamic properties of aerosols. It can change the surface
44
45 372 of particles, promote aggregation and influence the crystallinity of the spray-dried samples⁴⁴.
46
47 373 In this study, the residual water content was determined by using Karl Fisher titration. All
48
49 374 formulations had relatively low moisture content which followed the rank order of L-leucine
50
51 375 (4.11 ± 0.21%, w/w) < excipient-free (4.55 ± 0.49%, w/w) < lactose (5.8 ± 0.36%, w/w)
52
53 376 containing products. These results demonstrate that the optimized outlet air temperature
54
55
56
57
58
59
60

1
2
3 377 (around 65 °C) was suitable for serum albumin. The L-leucine containing formulation had the
4
5 378 lowest water content due to the low hygroscopic behavior of this amino acid^{46, 47}. The low
6
7 379 moisture content can potentially improve the flowability and consequently enhance lung
8
9
10 380 deposition due to reduced aggregation as expected. Storage conditions are also important, e.g.
11
12 381 the spray-dried amorphous lactose particles could transform into crystals easily in humidity
13
14 382 above 30%⁴⁸.

16 383 3.2.2. Fourier-Transform Infrared Spectroscopy (FT-IR)

18 384 FTIR analysis allows a quick and efficient identification of the compounds and by
19
20 385 their functional groups and bond vibrations. In the spectrum of raw Api, the following
21
22 386 characteristic regions were observed: 2710-2580 cm⁻¹ O-H bond, 1730-1680 cm⁻¹ C=O stretch
23
24 387 and 1450-1380 cm⁻¹ C-H bend. A broad peak observed at 3300 cm⁻¹ can be attributed to O-H
25
26 388 stretching and those bands at 1600-1400 cm⁻¹ (C-C stretch in ring) and 900-675 cm⁻¹ (C-H
27
28 389 'oop') can be assigned to the aromatic group (**Figure 4 A**). In the spectrum of BSA protein,
29
30 390 the amide I band at 1635 cm⁻¹ (mainly C=O stretch) and amide II band at 1530–1500 cm⁻¹ (C–
31
32 391 N stretching and N–H bend) can be seen. The medium broad peak at 3276 cm⁻¹ corresponds to
33
34 392 bonded N-H stretch of amide and a smaller band at 1057 cm⁻¹ is the C-N stretch of aliphatic
35
36 393 amine. In the spectra of the excipients-free formulation, the characteristic amide bands of
37
38 394 BSA can be seen and peak at 830 cm⁻¹ indicating the presence of Api (aromatic) which is an
39
40 395 indirect confirmation of Api encapsulation on BSA-NPs. Conformational changes can be
41
42 396 suggested due to the lack of the peak of aliphatic amine.

47 397 The spectra of raw Api, BSA, lactose and lactose containing product are displayed on **Figure**
48
49 398 **4 B**. In the spectra of lactose there is also a broad band around 3300 cm⁻¹ indicating the
50
51 399 stretching vibration of hydroxyl group. A weak band at 1654 cm⁻¹ is the bending vibration of
52
53 400 the crystalline water and peaks at 1200-1070 cm⁻¹ demonstrate the stretching vibration of C-
54
55 401 O-C in the glucose and galactose. The spectrum of amorphous lactose has the less number and
56
57
58
59
60

1
2
3 402 defined peaks and therefore it could be distinguished from the crystalline spectrum⁴⁹. The
4
5 403 characteristic broad band at 3300 cm⁻¹ in the spectrum of spray-dried product could originate
6
7 404 from the residual water content that is further supported by the Karl Fischer titration data
8
9
10 405 (lactose containing product had the highest water content). Similarly to the spectrum of
11
12 406 excipients-free formulation, the amide bands of BSA and a small peak of Api could be
13
14 407 observed. The peaks at 1200-1070 cm⁻¹ demonstrate the lactose content and the amorphous
15
16 408 state could be assumed.

17
18 409 Functional groups of L-leucine lead to its characteristic spectrum (**Figure 4 C**). The strong
19
20 410 band in the region of 2970-2910 cm⁻¹ can be accounted for the aliphatic C-H stretching. The
21
22 411 bonded N-H stretch is present in the region of 2600-2450 cm⁻¹. The NH₂ bending and the C-
23
24 412 N skeletal vibration appear in the regions of 1595-1550 cm⁻¹ and 1250-1020 cm⁻¹ ⁵⁰. The
25
26 413 presence of BSA characteristic peaks on the spray-dried formulation could be mainly
27
28 414 observed with and a small peak of Api but the major characteristic peaks of L-leucine are
29
30 415 obscured.

34 416 **3.2.3. X-ray powder diffraction (XRPD)**

35
36 417 XRPD is considered to be the most accurate method to study crystalline structure⁵¹.
37
38 418 The combined XRPD diffractograms of Api and spray-dried formulations are presented in
39
40 419 **Figure 5**. The characteristic narrow diffraction peaks of Api are due to the crystalline state of
41
42 420 the commercially available material. In comparison, broad diffuse peaks could be observed in
43
44 421 the diffractograms of the spray-dried formulations suggesting the amorphous state of BSA-
45
46 422 Api-NPs. The observed XRD patterns of spray-dried L-leucine and lactose were consistent
47
48 423 with literature^{48, 52, 53}.

51 424 **3.2.4. Differential scanning calorimetry analysis (DSC)**

52
53 425 The DSC curves of raw Api, excipients, physical mixtures and spray-dried
54
55 426 formulations were studied to examine crystallinity. As seen in **Figure 6**, there is only one
56
57
58
59
60

1
2
3 427 sharp endothermic peak at 360 °C indicating the melting point of raw Api; no impurities were
4
5 428 observed. Drug free albumin exhibited two broad peaks with onset values of 220 °C and 310
6
7 429 °C. The evaporation of residual water occurred at 50-120 °C. The melting point of Api on the
8
9 430 thermograms of raw material and physical mixtures corresponds to the crystalline habitus. In
10
11 431 the thermograms of physical mixtures on **Figure 6 B** the endothermic peak at 140 °C
12
13 432 indicating the crystalline lactose⁵⁴ and the sublimation of L-leucine crystals occurred at 200-
14
15 433 230 °C (**Figure 6 C**)⁵⁵. However, in each spray-dried formulation the absence of endotherms
16
17 434 confirms the loss of crystallinity. No peak could be observed around 360 °C indicating that
18
19 435 Api is in amorphous state due to the spray drying process which is in agreement with the
20
21 436 XRPD diffractograms. The amorphous form generated may result higher solubility of the
22
23 437 powders and dissolution of apigenin in lung fluids.

27 438 **3.2.5. Aerosol particle size analysis and redispersibility in water**

29 439 Dry powder formulations of BSA-Api-NPs were prepared with the aim of studying the
30
31 440 influence of excipients on the particle size and aerodynamic behavior. The deposition of
32
33 441 aerosols is significantly affected by particle size which should be small enough to pass
34
35 442 through the upper airways and large enough to avoid exhalation⁵⁶. Gravitational
36
37 443 sedimentation is the main driving force for deposition of a nanoparticulate system in the lung
38
39 444 due to the formation of aggregates in the micrometer size range. Particle geometry and surface
40
41 445 properties also play a significant role in reaching the bronchioles^{22,32}. It is well known that
42
43 446 particles can be deposited efficiently deeper in the lung if their aerodynamic diameter is in the
44
45 447 range of 1-5 µm and only those with 1-3 µm can reach the respiratory zone⁵⁷. Particles, larger
46
47 448 than 5 µm tend to deposit in the oropharynx and the mucociliary clearance plays a role in
48
49 449 clearing the particles towards the pharynx. However, very small particles, less than 1 µm are
50
51 450 usually exhaled because of the low inertia^{58,59}. Mucociliary clearance is the part of the natural
52
53 451 defense mechanism of the lung as well as the phagocytosis of macrophages in the alveolar
54
55
56
57
58
59
60

1
2
3 452 region. The aerosol particle size was determined by Sympatec HELOS laser diffractometer
4
5 453 (**Table 1**). The excipient-free and lactose containing products have similar sizes while spray
6
7 454 drying with L-leucine produced the smallest particles ($D_{50} = 2.473 \mu\text{m}$). In all cases, the
8
9 455 particle size could ensure the highest probability of delivery of apigenin into the respiratory
10
11 456 zone.

12
13
14 457 Following the re-dispersion of spray powders formulations in distilled water, the size of the
15
16 458 particles was preserved in the nanometer size range: without excipient ($358.9 \pm 5.3 \text{ nm}$, PDI:
17
18 459 0.315 ± 0.013), lactose ($366.1 \pm 4.8 \text{ nm}$, PDI: 0.382 ± 0.014) and L-leucine (343.7 ± 2.9 , PDI:
19
20 460 0.316 ± 0.011) containing products. The spray drying has no significant effect on the average
21
22 461 size of the particles suggesting the deposition of apigenin containing nanoparticles in the lung
23
24 462 fluid. Moreover, the excipients did not affect adversely the particle size.

25 26 27 463 **3.2.6. Solubility and Drug release studies of BSA-Api formulations**

28
29 464 The solubility of apigenin in nanoparticles was investigated in PBS buffer and mSLF
30
31 465 (**Figure 7 A**). The results showed that the solubility was slightly increased in mSLF media
32
33 466 (82-98% within 5 minutes), however, it was high in PBS buffer as well (79-95% within 5
34
35 467 minutes). These data indicated that the solubility of apigenin could be highly enhanced by
36
37 468 BSA nanoparticles in aqueous medium. Nevertheless, the dispersibility enhancers could play
38
39 469 a role in the solubility. In case of excipient free formulation, 91% of the encapsulated
40
41 470 apigenin was dissolved in mSLF within 5 minutes. Formulation prepared with lactose
42
43 471 increased the solubility rate up to 98%, however, it was slower (82%) when using L-leucine
44
45 472 and completed within 2 hours. These results could be attributed to the solubility of the
46
47 473 excipients themselves: lactose has very good water solubility, but L-leucine possess a low
48
49 474 solubility in water⁶⁰.

50
51
52 475 The apigenin release from the spray dried BSA-Api NPs was investigated with Franz
53
54 476 cell apparatus. It is a well known device for the dissolution of semisolid dosage forms and
55
56
57
58
59
60

1
2
3 477 approved by the USP (United States Pharmacopeia). However, there is no standardized
4
5 478 method for inhaled powders, Franz cell could be one of the alternative choices due to
6
7 479 simulating the diffusion controlled air-liquid interface of the lung. On the contrary, it has
8
9 480 some limitations such as small air bubbles under the contact area of membrane to dissolution
10
11 481 medium, wide range of standard deviation or the recovery usually around maximum 90% ⁶¹.
12
13 482 Based on the solubility measurements, mSLF was applied. The cumulative dissolution curves
14
15 483 of the prepared formulations are shown in **Figure 7 B**. As expected, the dissolution was
16
17 484 affected by the co-spray dried excipients. Lactose containing product resulted the fastest and
18
19 485 highest apigenin release due to the excellent water solubility. This enhancement of the
20
21 486 dissolution is supported by previously published data⁶². In contrast, the dissolution rate was
22
23 487 decreased when L-leucine was applied. The coating layer of L-leucine slowed down the
24
25 488 dissolution of apigenin which could be well observed in the dissolution curve. The low water
26
27 489 solubility of L-leucine is able to hinder the dissolution of the drug which was published
28
29 490 previously⁶⁰. These results suggest that the excipients play an important role in the solubility
30
31 491 and the dissolution as well.
32
33
34
35

36 492 **3.2.7. Aerosol delivery of BSA-Api formulations**

37
38 493 Particles can be taken up by alveolar macrophages which influences the therapeutic
39
40 494 outcome. Those nanoparticles which are soluble and above 200 nm are able to escape from
41
42 495 the macrophages therefore exhibit sustained therapeutic effect⁶³. The lung deposition and
43
44 496 therefore the efficacy of the inhaled therapeutics are governed by their aerosol properties⁵⁶.
45
46 497 Manufacturing respirable nanoparticles could be produced by aggregation in the favorable
47
48 498 size range or their incorporation into microparticles (1-5 μm) ²⁶. Lactose monohydrate is a
49
50 499 well-known, traditional carrier for improving the performance of inhaled products; however,
51
52 500 it is influenced by physicochemical properties and interaction with the active ingredient^{64, 65}.
53
54 501 It is the only FDA approved carrier and has also been shown to be a potential excipient for
55
56
57
58
59
60

1
2
3 502 protein encapsulation^{27, 65}. Recently, novel materials such as specific amino acids have been
4
5 503 developed for pulmonary formulations²⁶ and L-leucine is one of the most effective
6
7 504 dispersibility enhancer among them⁴⁷. Previous studies proved that 5% (w/w) L-leucine
8
9 505 improved the aerosol performance of raw naringin⁶⁶ and inclusion up to 15% (w/w) L-leucine
10
11 506 resulted higher ED and FPF of powder formulation of gentamicin⁴⁶.

12
13
14 507 In this study *in vitro* aerosol properties of three different dry powders formulations
15
16 508 were evaluated using the NGI which is regarded as an optimal instrument for analysis of
17
18 509 aerodynamic behavior of aerosol formulations for pulmonary drug delivery⁶⁷ according to
19
20 510 European and US Pharmacopeias. The obtained data and deposition pattern are presented in
21
22 511 **Table 2** and in **Figure 8**. It can be seen that more than 90% of apigenin could be recovered
23
24 512 from the NGI which is in the acceptable pharmacopeia range (75-125%). The ED ranged
25
26 513 between 91-96% indicating good flowability and high dispersibility of the powders. L-leucine
27
28 514 containing formulation had the highest ED as it could improve significantly the flowability of
29
30 515 the powders^{47, 53}. **Figure 8** shows the amount of Api deposited on the throat, device and
31
32 516 stages 1-7 expressed as a percentage of the total amount of recovered powder. All formulation
33
34 517 exhibited increased deposition in Stage 2 - 4 indicating enhanced drug delivery to the alveolar
35
36 518 regions. As expected, improved aerosol performance and deposition (Stage 3 and 4) could be
37
38 519 observed when L-leucine was used as an excipient. The FPF is one of the key parameters in
39
40 520 aerosol delivery and should be as high as possible⁶⁸. In this study, the FPF values ranged
41
42 521 between 58-66%, suggesting that the particles could be delivered into the peripheral regions.
43
44 522 Spray drying of nanoparticles in the presence of L-leucine resulted higher FPF value (66%)
45
46 523 due to the improved surface properties and morphology of the particles⁶⁵. In general, MMAD
47
48 524 values < 5 μm are for pulmonary lung delivery and between 2-3 μm are optimal for deep lung
49
50 525 deposition⁵⁶. In each case, the calculated mass median aerodynamic diameter (MMAD) data
51
52 526 were in agreement with the physical diameter size of the particles measured by laser
53
54
55
56
57
58
59
60

1
2
3 527 diffractometer. The data obtained ($< 5 \mu\text{m}$) support good dispersibility of the particles into the
4
5 528 lower airways and the deep lung. Therefore local delivery to the alveoli could be assured by
6
7 529 both excipient-free and lactose formulations generated (MMAD $3.2 \mu\text{m}$ and $3.1 \mu\text{m}$).
8
9 530 Moreover, formulation with L-leucine (MMAD $2.1 \mu\text{m}$) would be more optimal for deep lung
10
11 531 deposition. The size distribution of an aerosol is described best by GSD⁶⁹. Based on the GSD
12
13 532 data obtained, the L-leucine containing formulation had the narrowest size distribution (1.8
14
15 533 μm) but that of the others was also in the acceptable range ($< 3 \mu\text{m}$).
16
17 534 The overall values demonstrate that the particles of each dry powder nanoparticle formulation
18
19 535 are in the favorable aerodynamic size range, possess good dispersibility properties and
20
21 536 particle deposition. Therefore BSA-NPs is an attractive delivery system for pulmonary drug
22
23 537 delivery. We demonstrated that L-leucine improved better the aerosolization properties of
24
25 538 BSA-API-NPs than lactose monohydrate. Therefore it can be concluded that the use of
26
27 539 excipients influence the aerosol performance of nanoparticles.
28
29
30
31

32 **3.2.8. Particle morphology**

33
34 541 SEM analysis was conducted to investigate the morphology of the powders (**Figure 9**
35
36 542 **A and B**). It is well known that the morphology of the particles is strongly affected by the
37
38 543 solubility of the components and the nature of the excipients^{46,47}. The commercially available
39
40 544 Api was a crystalline powder featuring needle-shaped crystals. The excipient-free spray-dried
41
42 545 nanoparticles exhibited spherical shape and smooth or wrinkled surface. Particles of lactose
43
44 546 containing product had raisin-like surface and some of the particles were larger in accordance
45
46 547 with the laser diffraction particle size analysis. Powders prepared with L-leucine comprised
47
48 548 small and collapsed particles with strongly corrugated surface. The low aqueous solubility of
49
50 549 L-leucine leading to a shell on the surface of the droplet which interfere with the diffusion of
51
52 550 water therefore corrugated particles could form. This outcome was consistent with previous
53
54 551 observations^{46,53,70}. Corrugated surface improves the dispersibility of the dry powder
55
56
57
58
59
60

1
2
3 552 formulations and enhance respirability due to the reduced interparticulate cohesion (Van der
4
5 553 Waals forces) which is beneficial for particles intended for inhalation⁷¹.

554 **3.3. Antioxidant activity**

555 Owing to its reproducibility and comparability, the DPPH[•] assay is an established
556 method for investigating the antioxidant properties of natural compounds. Due to the H-
557 donating ability of the antioxidants, a stable reduced DPPH-H molecule can form. The
558 reaction can be seen visually and the detection can be carried out using UV-Vis
559 spectrophotometer^{72, 73}. Previous studies confirmed that Api is able to scavenge the DPPH[•]
560 free radical even in nanoscale delivery formulation^{74, 75}. In general, the scavenging activity is
561 influenced by concentration and structural features like hydrogen donating ability, position
562 and the degree of hydroxylation^{76, 77}. In order to calculate the exact concentration of
563 remaining DPPH[•] in the samples a calibration curve was plotted with $R^2=0.9999$. The time
564 required to reach the steady state was estimated to be 120 minutes, and the slow reaction
565 kinetic of Api has been reported⁷⁴. The discoloration of the deep purple DPPH[•] free radical
566 indicate the antioxidant properties of free and encapsulated Api. The inhibition of free
567 radicals by the prepared spray-dried formulations were compared to the empty BSA-NPs,
568 methanolic Api solution and “empty” nanoparticles (**Figure 10**). It can be seen that the free
569 and encapsulated Api have similar scavenging activity, moreover, the spray drying did not
570 result in the loss of scavenging activity. It has been reported that serum albumin is a
571 physiological circulating antioxidant in the body⁷⁸ which is confirmed by the inhibition
572 capacity of the empty BSA-NPs observed. Similar results were reported when encapsulating
573 rutin and keampferol⁷⁹ or quercetin¹⁷ where the antioxidant activity of the flavonoids are
574 retained by BSA. It can be concluded that the antioxidant activity of Api is preserved,
575 moreover, slightly enhanced by the BSA.

576 **4. CONCLUSION**

1
2
3 577 In this study novel apigenin containing albumin nanoparticles were prepared for
4
5 578 inhalation against lung injury caused by oxidative stress. Apigenin was recently classified as a
6
7 579 BCS II. drug with prominent antioxidant and anti-inflammatory properties in the lung. The
8
9
10 580 obtained results confirmed that incorporation of apigenin into the biocompatible albumin
11
12 581 nanoparticles resulted high encapsulation efficiency therefore it could be an attractive tool for
13
14 582 the delivery. Moreover, the spray dried nanoparticles possess good ability to re-disperse in
15
16 583 aqueous media and size of the particles was preserved in the nanometer size range. The
17
18 584 influence of dispersibility enhancers on the physicochemical properties and *in vitro*
19
20 585 pulmonary deposition were investigated and compared to the excipient-free formulation. The
21
22 586 obtained *in vitro* pulmonary depositions proved that the developed BSA-NP dry powders are
23
24 587 potentially able to carry apigenin deep in the lung, reaching the respiratory zone. The use of
25
26 588 novel excipient amino acid L-leucine resulted enhanced aerodynamic properties over the
27
28 589 traditional lactose monohydrate, indicating that the nature of the excipients and morphology
29
30 590 of the particles play a significant role in the formulation of nanoparticles for pulmonary
31
32 591 delivery. In addition, the solubility and dissolution characteristics of apigenin from
33
34 592 nanoparticles were determined in mSLF dissolution media, the co-spray dried excipients
35
36 593 played an important role. The dissolution rate was increased by the water soluble lactose and
37
38 594 decreased by L-leucine, which has low water solubility. Therefore the use of excipients should
39
40 595 be taken into consideration, may not required in case of albumin nanoparticles. We further
41
42 596 confirmed that the antioxidant activity is retained, thus the potential of albumin nanoparticles
43
44 597 as an effective pulmonary delivery system for flavonoids such as apigenin.

49 **ACKNOWLEDGEMENTS**

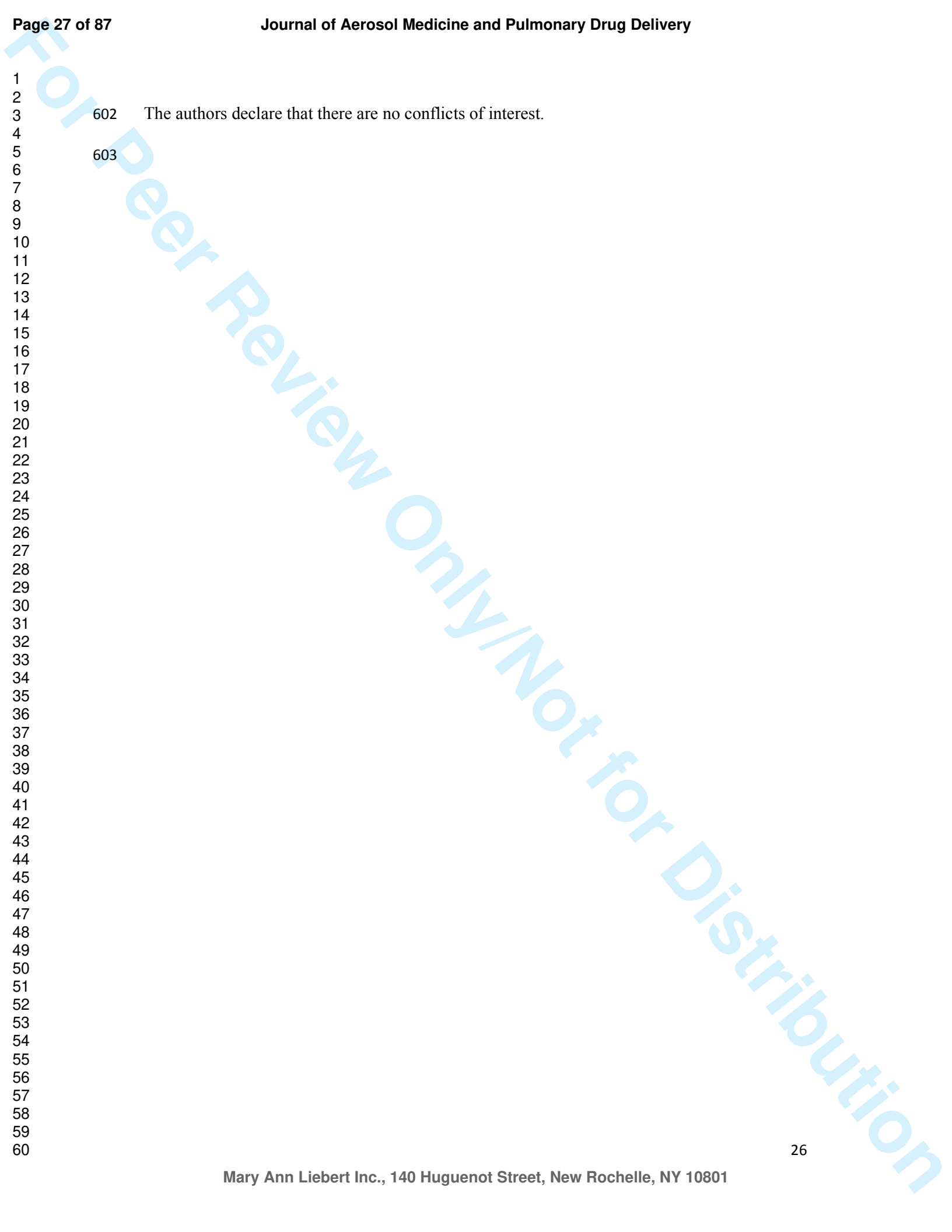
50
51
52 599 The authors gratefully acknowledge to Róbert Kovács for providing the SEM pictures at
53
54 600 Budapest University of Technology and Economics.

56 601 **Author Disclosure Statement**

1
2
3
4
5
6
7
8
9
10
11
12
13
14
15
16
17
18
19
20
21
22
23
24
25
26
27
28
29
30
31
32
33
34
35
36
37
38
39
40
41
42
43
44
45
46
47
48
49
50
51
52
53
54
55
56
57
58
59
60

602 The authors declare that there are no conflicts of interest.

603



604 REFERENCES

- 605 1. Chow C-W, Herrera Abreu MT, Suzuki T, and Downey GP. Oxidative Stress and
606 Acute Lung Injury. *Am J Respir Cell Mol Biol.* 2003;29:427-431.
- 607 2. Chen XW, Serag ES, Sneed KB, and Zhou SF. Herbal bioactivation, molecular targets
608 and the toxicity relevance. *Chem Biol Interact.* 2011;192:161-176.
- 609 3. Patel D, Shukla S, and Gupta S. Apigenin and cancer chemoprevention: progress,
610 potential and promise (review). *Int J Oncol.* 2007;30:233-245.
- 611 4. Kim SJ, Jeong HJ, Moon PD, Lee KM, Lee HB, Jung HJ, Jung SK, Rhee HK, Yang
612 DC, Hong SH, and Kim HM. Anti-inflammatory activity of gumiganghwaltang
613 through the inhibition of nuclear factor-kappa B activation in peritoneal macrophages.
614 *Biol Pharm Bull.* 2005;28:233-237.
- 615 5. Kowalski J, Samojedny A, Paul M, Pietsz G, and Wilczok T. Effect of apigenin,
616 kaempferol and resveratrol on the expression of interleukin-1beta and tumor necrosis
617 factor-alpha genes in J774.2 macrophages. *Pharmacol Rep.* 2005;57:390-394.
- 618 6. Lee J-H, Zhou H, Cho S, Kim Y, Lee Y, and Jeong C. Anti-inflammatory mechanisms
619 of apigenin: inhibition of cyclooxygenase-2 expression, adhesion of monocytes to
620 human umbilical vein endothelial cells, and expression of cellular adhesion molecules.
621 *Archives of Pharmacal Research.* 2007;30:1318-1327.
- 622 7. Chen L and Zhao WEI. Apigenin protects against bleomycin-induced lung fibrosis in
623 rats. *Exp Ther Med.* 2016;11:230-234.
- 624 8. Luan RL, Meng XX, and Jiang W. Protective Effects of Apigenin Against Paraquat-
625 Induced Acute Lung Injury in Mice. *Inflammation.* 2016; 39:752-758.
- 626 9. Basios N, Lampropoulos P, Papalois A, Lambropoulou M, Pitiakoudis MK, Kotini A,
627 Simopoulos C, and Tsaroucha AK. Apigenin Attenuates Inflammation in

- 1
2
3 628 Experimentally Induced Acute Pancreatitis-Associated Lung Injury. *J Invest Surg.*
4
5 629 2015;2:1-7.
6
7 630 **10.** Patil R, Babu RL, Naveen Kumar M, Kiran Kumar KM, Hegde S, Ramesh G, and
8
9 631 Chidananda Sharma S. Apigenin inhibits PMA-induced expression of pro-
10
11 632 inflammatory cytokines and AP-1 factors in A549 cells. *Mol Cell Biochem.*
12
13 633 2015;403:95-106.
14
15
16 634 **11.** Wang J, Liu Y-T, Xiao L, Zhu L, Wang Q, and Yan T. Anti-Inflammatory Effects of
17
18 635 Apigenin in Lipopolysaccharide-Induced Inflammation in Acute Lung Injury by
19
20 636 Suppressing COX-2 and NF- κ B Pathway. *Inflammation.* 2014;37:2085-2090.
21
22
23 637 **12.** Zhang J, Liu D, Huang Y, Gao Y, and Qian S. Biopharmaceutics classification and
24
25 638 intestinal absorption study of apigenin. *Int J Pharm.* 2012;436:311-317.
26
27 639 **13.** Ajazuddin and Saraf S. Applications of novel drug delivery system for herbal
28
29 640 formulations. *Fitoterapia.* 2010;81:680-689.
30
31 641 **14.** Elzoghby AO, Samy WM, and Elgindy NA. Albumin-based nanoparticles as potential
32
33 642 controlled release drug delivery systems. *J Control Release.* 2012;157:168-182.
34
35
36 643 **15.** Hu Y-J, Liu Y, Sun T-Q, Bai A-M, Lü J-Q, and Pi Z-B. Binding of anti-inflammatory
37
38 644 drug cromolyn sodium to bovine serum albumin. *Int J Biol Macromolec.* 2006;39:280-
39
40 645 285.
41
42
43 646 **16.** Fasano M, Curry S, Terreno E, Galliano M, Fanali G, Narciso P, Notari S, and
44
45 647 Ascenzi P. The extraordinary ligand binding properties of human serum albumin.
46
47 648 *IUBMB Life.* 2005;57:787-796.
48
49 649 **17.** Fang R, Hao R, Wu X, Li Q, Leng X, and Jing H. Bovine Serum Albumin
50
51 650 Nanoparticle Promotes the Stability of Quercetin in Simulated Intestinal Fluid. *J Agr*
52
53 651 *Food Chem.* 2011;59:6292-6298.
54
55
56
57
58
59
60

- 1
2
3 652 **18.** He X, Xiang N, Zhang J, Zhou J, Fu Y, Gong T, and Zhang Z. Encapsulation of
4
5 653 teniposide into albumin nanoparticles with greatly lowered toxicity and enhanced
6
7 654 antitumor activity. *Int J Pharm.* 2015;487:250-259.
- 8
9
10 655 **19.** Muralidharan P, Malapit M, Mallory E, Hayes Jr D, and Mansour HM. Inhalable
11
12 656 nanoparticulate powders for respiratory delivery. *Nanomedicine: NBM.* 2015;11:1189-
13
14 657 1199.
- 15
16 658 **20.** Malcolmson RJ and Embleton JK. Dry powder formulations for pulmonary delivery.
17
18 659 *Pharm Sci Technol To.* 1998;1:394-398.
- 19
20
21 660 **21.** Stegemann S, Kopp S, Borchard G, Shah VP, Senel S, Dubey R, Urbanetz N, Cittero
22
23 661 M, Schoubben A, Hippchen C, Cade D, Fuglsang A, Morais J, Borgström L, Farshi F,
24
25 662 Seyfang KH, Hermann R, van de Putte A, Klebovich I, and Hincal A. Developing and
26
27 663 advancing dry powder inhalation towards enhanced therapeutics. *Eur J Pharm Sci.*
28
29 664 2013;48:181-194.
- 30
31
32 665 **22.** Yang W, Peters JI, and Williams Iii RO. Inhaled nanoparticles—A current review. *Int*
33
34 666 *J Pharm.* 2008;356:239-247.
- 35
36 667 **23.** Geiser M. Update on macrophage clearance of inhaled micro- and nanoparticles. *J*
37
38 668 *Aerosol Med Pulm Drug Deliv.* 2010;23:207-217.
- 39
40
41 669 **24.** Woods A, Patel A, Spina D, Riffo-Vasquez Y, Babin-Morgan A, de Rosales RT,
42
43 670 Sunassee K, Clark S, Collins H, Bruce K, Dailey LA, and Forbes B. In vivo
44
45 671 biocompatibility, clearance, and biodistribution of albumin vehicles for pulmonary
46
47 672 drug delivery. *J Control Release.* 2015;210:1-9.
- 48
49
50 673 **25.** Swarbrick J. *Encyclopedia of Pharmaceutical Technology.* Informa
51
52 674 Healthcare:London; 2007; 671 - 1434.
- 53
54 675 **26.** Mansour HM, Rhee YS, and Wu X. Nanomedicine in pulmonary delivery. *Int J*
55
56 676 *Nanomedicine.* 2009;4:299-319.

- 1
2
3 677 27. Shoyele SA and Cawthorne S. Particle engineering techniques for inhaled
4
5 678 biopharmaceuticals. *Adv Drug Deliv Rev.* 2006;58:1009-1029.
6
7 679 28. Sung JC, Pulliam BL, and Edwards DA. Nanoparticles for drug delivery to the lungs.
8
9 680 *Trends Biotechnol.* 2007;25:563-570.
10
11 681 29. Desai NP, Tao C, Yang A, Louie L, Yao Z, Soon-Shiong P, and Magdassi S. Protein
12
13 682 stabilized pharmacologically active agents, methods for the preparation thereof and
14
15 683 methods for the use thereof. Google Patents, 2004. US6749868 B1
16
17 684 30. Son YJ, McConville JT. Development of a standardized dissolution test method for
18
19 685 inhaled pharmaceutical formulations. *Int J Pharm.* 2009;382:15–22.
20
21 686 31. Hatano T. KH, Yasuhara T., Okuda T. 2 new flavonoids and other constituents in
22
23 687 licorice root-their relative astringency and radical scavenging effects. *Chem Pharm*
24
25 688 *Bull.* 1988;36:2090-2097.
26
27 689 32. Paranjpe M and Muller-Goymann CC. Nanoparticle-mediated pulmonary drug
28
29 690 delivery: a review. *Int J Mol Sci.* 2014;15:5852-5873.
30
31 691 33. Kim TH, Jiang HH, Youn YS, Park CW, Tak KK, Lee S, Kim H, Jon S, Chen X, and
32
33 692 Lee KC. Preparation and characterization of water-soluble albumin-bound curcumin
34
35 693 nanoparticles with improved antitumor activity. *Int J Pharm.* 2011;403:285-291.
36
37 694 34. Wei Y, Li L, Xi Y, Qian S, Gao Y, and Zhang J. Sustained release and enhanced
38
39 695 bioavailability of injectable scutellarin-loaded bovine serum albumin nanoparticles. *Int*
40
41 696 *J Pharm.* 2014;476:142-148.
42
43 697 35. Valeur B. *Molecular fluorescence principles and applications.* Wiley-VCH:
44
45 698 Weinheim; 2002; 73-124.
46
47 699 36. Yuan J-L, lv Z, Liu Z-G, Hu Z, and Zou G-L. Study on interaction between apigenin
48
49 700 and human serum albumin by spectroscopy and molecular modeling. *J Photochem*
50
51 701 *Photobiol A.* 2007;191:104-113.
52
53
54
55
56
57
58
59
60

- 1
2
3 702 37. Naveenraj S and Anandan S. Binding of serum albumins with bioactive substances –
4
5 703 Nanoparticles to drugs. *J Photochem Photobiol C*. 2013;14:53-71.
6
7 704 38. Tayeh N, Rungassamy T, and Albani JR. Fluorescence spectral resolution of
8
9 705 tryptophan residues in bovine and human serum albumins. *J Pharm Biomed Anal*.
10
11 706 2009;50:107-116.
12
13 707 39. Zhao X-N, Liu Y, Niu L-Y, and Zhao C-P. Spectroscopic studies on the interaction of
14
15 708 bovine serum albumin with surfactants and apigenin. *Spectrochim Acta A Mol Biomol*
16
17 709 *Spectrosc*. 2012;94:357-364.
18
19 710 40. Lin C-Z, Hu M, Wu A-Z, and Zhu C-C. Investigation on the differences of four
20
21 711 flavonoids with similar structure binding to human serum albumin. *J Pharm Anal*.
22
23 712 2014;4:392-398.
24
25 713 41. Cao H, Liu Q, Shi J, Xiao J, and Xu M. Comparing the Affinities of Flavonoid
26
27 714 Isomers with Protein by Fluorescence Spectroscopy. *Anal Lett*. 2008;41:521-532.
28
29 715 42. Shang Y and Li H. Studies of the interaction between apigenin and bovine serum
30
31 716 albumin by spectroscopic methods. *Russ J Gen Chem*. 2010;80:1710-1717.
32
33 717 43. Tang L, Jia W, and Zhang D. The effects of experimental conditions of fluorescence
34
35 718 quenching on the binding parameters of apigenin to bovine serum albumin by
36
37 719 response surface methods. *Luminescence*. 2014;29:344-351.
38
39 720 44. Stahl K, Claesson M, Lilliehorn P, Linden H, and Backstrom K. The effect of process
40
41 721 variables on the degradation and physical properties of spray dried insulin intended for
42
43 722 inhalation. *Int J Pharm*. 2002;233:227-237.
44
45 723 45. Jensen DM, Cun D, Maltesen MJ, Frokjaer S, Nielsen HM, and Foged C. Spray drying
46
47 724 of siRNA-containing PLGA nanoparticles intended for inhalation. *J Control Release*.
48
49 725 2010;142:138-145.
50
51
52
53
54
55
56
57
58
59
60

- 1
2
3 726 46. Aquino RP, Prota L, Auriemma G, Santoro A, Mencherini T, Colombo G, and Russo
4
5 727 P. Dry powder inhalers of gentamicin and leucine: formulation parameters, aerosol
6
7 728 performance and in vitro toxicity on CuFi1 cells. *Int J Pharm.* 2012;426:100-107.
8
9
10 729 47. Yang X-F, Xu Y, Qu D-S, and Li H-Y. The influence of amino acids on aztreonam
11
12 730 spray-dried powders for inhalation. *Asian J Pharm Sci.* 2015;10:541-548.
13
14 731 48. Wu L, Miao X, Shan Z, Huang Y, Li L, Pan X, Yao Q, Li G, and Wu C. Studies on
15
16 732 the spray dried lactose as carrier for dry powder inhalation. *Asian J Pharm Sci.*
17
18 733 2014;9:336-341.
19
20 734 49. Listiohadi Y, Hourigan J, Sleigh R, and Steele R. Thermal analysis of amorphous
21
22 735 lactose and α -lactose monohydrate. *Dairy Sci Technol.* 2009;89:43-67.
23
24
25 736 50. Němec I and Mička Z. FTIR and FT Raman study of L-leucine addition compound
26
27 737 with nitric acid. *J Mol Struct.* 1999;482-483:23-28.
28
29
30 738 51. Newman AW and Byrn SR. Solid-state analysis of the active pharmaceutical
31
32 739 ingredient in drug products. *Drug Discov Today.* 2003;8:898-905.
33
34 740 52. Sou T, Kaminskis LM, Nguyen T-H, Carlberg R, McIntosh MP, and Morton DAV.
35
36 741 The effect of amino acid excipients on morphology and solid-state properties of multi-
37
38 742 component spray-dried formulations for pulmonary delivery of biomacromolecules.
39
40 743 *Eur J Pharm Biopharm.* 2013;83:234-243.
41
42
43 744 53. Mangal S, Meiser F, Tan G, Gengenbach T, Denman J, Rowles MR, Larson I, and
44
45 745 Morton DAV. Relationship between surface concentration of l-leucine and bulk
46
47 746 powder properties in spray dried formulations. *Eur J Pharm Biopharm.* 2015;94:160-
48
49 747 169.
50
51
52 748 54. Gombás Á, Szabó-Révész P, Kata M, Regdon G, Jr., and Erős I. Quantitative
53
54 749 Determination of Crystallinity of α -Lactose Monohydrate by DSC. *J Therm Anal*
55
56 750 *Calorim.* 2002;68:503-510.
57
58
59
60

- 1
2
3 751 **55.** Raula J, Seppälä J, Malm J, Karppinen M, and Kauppinen EI. Structure and
4
5 752 Dissolution of l-Leucine-Coated Salbutamol Sulphate Aerosol Particles. *AAPS*
6
7 753 *PharmSciTech*. 2012;13:707-712.
8
9
10 754 **56.** Yang MY, Chan JGY, and Chan H-K. Pulmonary drug delivery by powder aerosols. *J*
11
12 755 *Control Release*. 2014;193:228-240.
13
14 756 **57.** Chow AL, Tong HY, Chattopadhyay P, and Shekunov B. Particle Engineering for
15
16 757 Pulmonary Drug Delivery. *Pharm Res*. 2007;24:411-437.
17
18 758 **58.** Liang Z, Ni R, Zhou J, and Mao S. Recent advances in controlled pulmonary drug
19
20 759 delivery. *Drug Discov To*. 2015;20:380-389.
21
22
23 760 **59.** Heyder J, Gebhart J, Rudolf G, Schiller CF, and Stahlhofen W. Deposition of particles
24
25 761 in the human respiratory tract in the size range 0.005–15 μm . *J Aerosol Sci*.
26
27 762 1986;17:811-825.
28
29 763 **60.** Raula J, Seppälä J, Malm J, Karppinen M, Kauppinen EI. Structure and dissolution of
30
31 764 L-leucine-coated salbutamol sulphate aerosol particles. *AAPS PharmSciTech*. 2012;
32
33 765 13:707-12.
34
35 766 **61.** May S, Jensen B, Wolkenhauer M, Schneider M, Lehr CM. Dissolution techniques for
36
37 767 in vitro testing of dry powders for inhalation. *Pharm Res*. 2012;29:2157-66.
38
39 768 **62.** Knieke C, Azad MA, To D, Bilgili E, Davé RN. Sub-100 micron fast dissolving
40
41 769 nanocomposite drug powders. *Powder Technol*. 2015;271:49–60.
42
43
44 770 **63.** Patel B, Gupta N, and Ahsan F. Particle engineering to enhance or lessen particle
45
46 771 uptake by alveolar macrophages and to influence the therapeutic outcome. *Eur J*
47
48 772 *Pharm Biopharm*. 2015;89:163-174.
49
50 773 **64.** Kou X, Chan LW, Steckel H, and Heng PWS. Physico-chemical aspects of lactose for
51
52 774 inhalation. *Adv Drug Deliv Rev*. 2012;64:220-232.
53
54
55 775 **65.** Pilcer G, Wauthoz N, and Amighi K. Lactose characteristics and the generation of the
56
57 776 aerosol. *Adv Drug Deliv Rev*. 2012;64:233-256.
58
59
60

- 1
2
3 777 66. Prota L, Santoro A, Bifulco M, Aquino RP, Mencherini T, and Russo P. Leucine
4
5 778 enhances aerosol performance of Naringin dry powder and its activity on cystic
6
7 779 fibrosis airway epithelial cells. *Int J Pharm.* 2011;412:8-19.
8
9
10 780 67. Taki M, Marriott C, Zeng X-M, and Martin GP. Aerodynamic deposition of
11
12 781 combination dry powder inhaler formulations in vitro: A comparison of three
13
14 782 impactors. *Int J Pharm.* 2010;388:40-51.
15
16 783 68. Davis SS. Delivery of peptide and non-peptide drugs through the respiratory tract.
17
18 784 *Pharm Sci Techn To.* 1999;2:450-456.
19
20 785 69. Musante CJ, Schroeter JD, Rosati JA, Crowder TM, Hickey AJ, and Martonen TB.
21
22 786 Factors affecting the deposition of inhaled porous drug particles. *J Pharm Sci.*
23
24 787 2002;91:1590-1600.
25
26 788 70. Lechuga-Ballesteros D, Charan C, Stults CL, Stevenson CL, Miller DP, Vehring R,
27
28 789 Tep V, and Kuo MC. Trileucine improves aerosol performance and stability of spray-
29
30 790 dried powders for inhalation. *J Pharm Sci.* 2008;97:287-302.
31
32 791 71. Chew NY and Chan HK. The role of particle properties in pharmaceutical powder
33
34 792 inhalation formulations. *J Aerosol Med.* 2002;15:325-330.
35
36 793 72. Brand-Williams W, Cuvelier ME, and Berset C. Use of a free radical method to
37
38 794 evaluate antioxidant activity. *LWT - Food Science and Technology.* 1995;28:25-30.
39
40 795 73. Villaño D, Fernández-Pachón MS, Moyá ML, Troncoso AM, and García-Parrilla MC.
41
42 796 Radical scavenging ability of polyphenolic compounds towards DPPH[•] free radical.
43
44 797 *Talanta.* 2007;71:230-235.
45
46 798 74. Al Shaal L, Shegokar R, and Muller RH. Production and characterization of
47
48 799 antioxidant apigenin nanocrystals as a novel UV skin protective formulation. *Int J*
49
50 800 *Pharm.* 2011;420:133-140.
51
52
53
54
55
56
57
58
59
60

- 1
2
3 801 75. Papay Z.E AI. Study on the antioxidant activity during the formulation of biological
4
5 802 active ingredient. *European Scientific Journal*. 2014;Special Edition 3:252-257.
6
7 803 76. Yang J, Guo J, and Yuan J. In vitro antioxidant properties of rutin. *LWT - Food*
8
9 804 *Science and Technology*. 2008;41:1060-1066.
10
11 805 77. Natella F, Nardini M, Di Felice M, and Scaccini C. Benzoic and Cinnamic Acid
12
13 806 Derivatives as Antioxidants: Structure–Activity Relation. *J Agr Food Chem*.
14
15 807 1999;47:1453-1459.
16
17
18 808 78. Roche M, Rondeau P, Singh NR, Tarnus E, and Bourdon E. The antioxidant properties
19
20 809 of serum albumin. *FEBS Lett*. 2008;582:1783-1787.
21
22
23 810 79. Fang R, Jing H, Chai Z, Zhao G, Stoll S, Ren F, Liu F, and Leng X. Study of the
24
25 811 physicochemical properties of the BSA: flavonoid nanoparticle. *Eur Food Res*
26
27 812 *Technol*. 2011;233:275-283.
28
29
30
31 813
32
33 814
34
35
36
37
38
39
40
41
42
43
44
45
46
47
48
49
50
51
52
53
54
55
56
57
58
59
60

815 TABLES

816 Table 1

817 Aerosol particle sizes of spray-dried nanoparticles with Sympatec HELOS laser
818 diffractometer in μm .

	Excipient-free	Lactose	L-leucine
ED (%)	91.862 ± 2.735	93.950 ± 1.046	95.183 ± 0.667
FPF (%)	65.617 ± 3.422	58.463 ± 6.031	66.090 ± 2.777
MMAD (μm)	3.210 ± 0.069	3.130 ± 0.001	2.123 ± 0.098
GSD (μm)	2.823 ± 0.113	2.270 ± 0.212	1.887 ± 0.063
RD (%)	99.1 ± 5.012	94.7 ± 4.091	96.3 ± 2.161

819

820

821 Table 2

822 Aerodynamic characteristic of spray-dried nanoparticles.

	Excipient-free	Lactose	L-leucine
D ₁₀	1.033 ± 0.032	1.020 ± 0.070	0.843 ± 0.680
D ₅₀	3.030 ± 0.092	3.107 ± 0.102	2.473 ± 0.300
D ₉₀	7.110 ± 0.306	7.117 ± 0.337	5.287 ± 0.670

823

824

825 **FIGURE CAPTIONS**

826 **Figure 1.** Molecular structure of apigenin.

827 **Figure 2.** Fluorescence emission spectra of BSA solution, BSA nanoparticles and BSA-Api
828 nanoparticles. The excitation wavelength was set to 285 nm (EM: emission, EXC:
829 excitation)

830 **Figure 3.** Three dimensional fluorescence emission maps and two dimensional contour
831 maps of empty BSA nanoparticles and BSA-Api nanoparticles. Color scale
832 displays the range of observed fluorescence intensities.

833 **Figure 4. A)** FT-IR spectra of apigenin (1), BSA (2) and the excipient-free spray-dried
834 BSA-Api nanoparticles (3).

835 **B)** FT-IR spectra of apigenin (1), BSA (2), lactose (3) and the spray-dried BSA-
836 Api nanoparticles with lactose (4).

837 **C)** FT-IR spectra of apigenin (1), BSA (2), L-leucine (3) and the spray-dried
838 BSA-Api nanoparticles with L-leucine (4).

839 **Figure 5.** XRPD diffraction pattern of raw apigenin and the formulations.

840 **Figure 6. A)** DSC thermograms of apigenin (1), BSA (2) physical mixture (3) and the
841 excipient-free spray dried BSA-Api nanoparticles (4).

842 **B)** DSC spectra of apigenin (1), BSA (2), physical mixture (3) and the spray-dried
843 BSA-Api nanoparticles with lactose (4).

844 **C)** DSC spectra of apigenin (1), BSA (2), physical mixture (3) and the spray-dried
845 BSA-Api nanoparticles with L-leucine (4).

846 **Figure 7. A)** Solubility of spray dried BSA-Api formulations in PBS buffer and modified
847 simulated lung fluid (mSLF).

848 **B)** Dissolution of apigenin from the formulations as a function of time in modified
849 simulated lung fluid (mSLF).

1
2
3 850 **Figure 8.** NGI deposition pattern of the spray dried BSA-Api formulations.

4 851 **Figure 9.** SEM images of raw apigenin (1), excipient-free spray dried BSA-Api
5
6 852 nanoparticles (2), spray-dried BSA-Api nanoparticles with lactose (3), spray-dried
7
8 853 BSA-Api nanoparticles with L-leucine (4) 20000 x magnification.

9
10
11 854 **Figure 10.** Radical scavenging activity of Apigenin solution, empty BSA nanoparticles,
12
13 855 BSA-Apigenin nanoparticles (NP) and spray-dried nanoparticles (SD) with
14
15 856 excipients. The antioxidant activity is expressed as the inhibition of DPPH[•] free
16
17 857 radical in percent.

18
19
20 858 **To whom correspondence should be addressed:**

21
22 859 antal.istvan@pharma.semmelweis-univ.hu

23
24 860 Department of Pharmaceutics

25
26 861 Semmelweis University

27
28 862 Hőgyes E. Street 7-9,

29
30 863 H-1092 Budapest, Hungary

31
32 864 Tel/Fax: +3612017-0914; Tel.: +361476-3600/53066, 53087

33
34
35 865
36
37
38
39
40
41
42
43
44
45
46
47
48
49
50
51
52
53
54
55
56
57
58
59
60

1
2
3 1 **Study on the pulmonary delivery system of apigenin loaded albumin**
4
5 2 **nanocarriers with antioxidant activity**
6

7
8 3 Zsófia Edit Pápay¹, Annamária Kósa, PhD², Béla Böddi, PhD², Zahra Merchant³, Imran Y
9 4 Saleem, PhD⁴, Mohammed Gulrez Zariwala, PhD⁵, Imre Klebovich, PhD¹, Satyanarayana
10 5 Somavarapu, PhD^{3*}, István Antal, PhD^{1*}
11

12
13 6 ¹ Department of Pharmaceutics, Semmelweis University, Hőgyes E. Street 7-9, H-1092
14 7 Budapest, Hungary
15

16
17 8 ² Department of Plant Anatomy, Institute of Biology, Eötvös Lóránd University, Pázmány
18 9 Péter Street 1/C, Budapest, Hungary
19

20
21 10 ³ Department of Pharmaceutics, UCL School of Pharmacy, 29-39 Brunswick Square, London
22 11 WC1N 1AX, United Kingdom
23

24
25 12 ⁴ Formulation and Drug Delivery Research, School of Pharmacy and Biomolecular Sciences,
26 13 Liverpool John Moores University, Liverpool, United Kingdom
27

28
29 14 ⁵ Department of Biomedical Science, Faculty of Science and Technology, University of
30 15 Westminster, 115 New Cavendish Street, London, W1W 6UW, United Kingdom
31

32
33 16 * To whom correspondence should be addressed:
34

35
36 17 antal.istvan@pharma.semmelweis-univ.hu
37

38
39 18 Department of Pharmaceutics
40

41 19 Semmelweis University
42

43 20 Hőgyes E. Street 7-9,
44

45 21 H-1092 Budapest, Hungary
46

47 22 Tel/Fax: +3612017-0914; Tel.: +361476-3600/53066, 53087
48

49 23 **Running title:**
50

51 24 **Albumin-Apigenin Nanoparticles against Lung Injury**
52

53 25
54
55
56
57
58
59
60

ABSTRACT

Background: Respiratory diseases are mainly derived from acute and chronic inflammation of the alveoli and bronchi. The pathophysiological mechanisms of pulmonary inflammation mainly arise from oxidative damage that could ultimately lead to acute lung injury (ALI). Apigenin (Api) is a natural polyphenol with prominent antioxidant and anti-inflammatory properties in the lung. Inhalable formulations consist of nanoparticles (NPs) have several advantages over other administration routes therefore this study investigated the application of apigenin loaded bovine serum albumin nanoparticles (BSA-Api-NPs) for pulmonary delivery.

Methods: Dry powder formulations of BSA-Api-NPs were prepared by spray drying and characterized by laser diffraction particle sizing, scanning electron microscopy, differential scanning calorimetry and powder X-ray diffraction. The influence of dispersibility enhancers (lactose monohydrate and L-leucine) on the *in vitro* aerosol deposition using a next generation impactor (NGI) was investigated in comparison to excipient-free formulation. The dissolution of Api was determined in simulated lung fluid by using Franz cell apparatus. The antioxidant activity was determined by 2,2-Diphenyl-1-picrylhydrazyl (DPPH') free radical scavenging assay.

Results: The encapsulation efficiency and the drug loading was measured to be $82.61 \pm 4.56\%$ and $7.51 \pm 0.415\%$. The optimized spray drying conditions were suitable to produce particles with low residual moisture content. The spray dried BSA-Api-NPs possessed good the aerodynamic properties due to small and wrinkled particles with low mass median aerodynamic diameter, high emitted dose and fine particle fraction. The aerodynamic properties was enhanced by leucine and decreased by lactose, however, the dissolution was reversely affected. The DPPH' assay confirmed that the antioxidant activity of encapsulated Api was preserved.

1
2
3 49 **Conclusion:** This study provides evidence to support that albumin nanoparticles are suitable
4
5 50 carriers of Api and the use of traditional or novel excipients should be taken into
6
7 51 consideration. The developed BSA-Api-NPs is a novel delivery system against lung injury
8
9
10 52 with potential antioxidant activity.

11 53 **Keywords:** aerosol distribution, inhaled therapy, modeling

12
13
14 54
15
16
17
18
19
20
21
22
23
24
25
26
27
28
29
30
31
32
33
34
35
36
37
38
39
40
41
42
43
44
45
46
47
48
49
50
51
52
53
54
55
56
57
58
59
60

1. INTRODUCTION

Respiratory diseases are thought to be mainly derived from acute and chronic inflammation of the alveoli and the bronchi. The pathophysiological mechanisms of pulmonary inflammation arise from several factors, including oxidative damage due to cytotoxic mediators that may ultimately lead to acute lung injury (ALI), acute respiratory distress syndrome (ARDS) and cancer¹. A growing body of scientific data suggests that natural occurring compounds possess preventive and therapeutic properties with inherent low toxicity². Among phytochemicals, apigenin (Api, **Figure 1**) is a promising candidate as a therapeutic agent, mainly due to its antioxidant and anti-inflammatory properties³⁻⁶. It has been demonstrated that Api has protective effects against bleomycin-induced lung fibrosis in rats which is associated with its antioxidant and anti-inflammatory capacities⁷. Another study provided evidence that Api has been able to decrease oxidative stress and inflammation on paraquat-induced ALI in mice⁸ and reduced the pathological alterations of pulmonary tissue in acute pancreatitis associated ALI, therefore suggesting protection in the lung⁹. Furthermore, Api has anti-inflammatory effect owing to significant inhibition of pro-inflammatory cytokines, activator protein (AP-1) and cyclooxygenase-2 (COX-2) in human pulmonary epithelial cells¹⁰ and in mice as well¹¹. However, Api's has low water solubility (2.16 µg/ml at pH 7.5) and therefore it was recently classified as BCS (Biopharmaceutical Classification System) II. drug¹².

Encapsulation and delivery of phytoconstituents with health effects has attracted much attention in recent years. Developing a suitable carrier system is essential to improve the overall activity and reduce the possible toxicity of these agents¹³. Among the potential carrier systems, serum albumin nanoparticles have notable advantages including biodegradability, non-antigenicity and cell-targeting ability^{14,15}. Moreover, albumin provide exceptional ligand binding capacity for various drugs owing to three homologous domains with two separate

1
2
3 80 helical subdomains¹⁶. Studies reported the successful incorporation of flavonoids into albumin
4
5 81 nanoparticles that can improve their stability¹⁷ and antitumor activity¹⁸.
6

7
8 82 Pulmonary delivery of pharmacologically active ingredients are extensively studied due to
9
10 83 prominent advantages over other delivery routes of administration¹⁹. The lungs have a large
11
12 84 surface area, limited enzymatic activity and high permeability therefore drugs can be
13
14 85 delivered either locally for the treatment of respiratory diseases or systematically in order to
15
16 86 e.g. avoid first pass metabolism²⁰. Dry Powder Inhaler (DPI) products offer precise and
17
18 87 reproducible delivery of fine drug particle fraction to the deep lung and recent studies have
19
20 88 proved that these are more cost effective than other products²¹. This non-invasive delivery
21
22 89 route could be suitable for poorly water soluble drugs in nanoparticles with increased
23
24 90 solubility²². It is also well recognized that nanoparticles have benefits over other carriers in
25
26 91 the micron scale such as controlled drug release, avoiding mucociliary clearance and improve
27
28 92 deposition^{23, 24}. Albumin is naturally present in the body, as well as in the lung epithelium²⁴,
29
30 93 moreover, the body can absorb proteins into the bloodstream by transcytosis which occurs
31
32 94 deep in the lung and allows drug molecules to pass through cell membrane²⁵. Therefore the
33
34 95 presence of BSA in the nanoparticle system increases membrane permeability, may facilitate
35
36 96 epithelial cell uptake and translocation through the alveo-capillary barrier of the lung²⁶. It
37
38 97 was proved that albumin nanoparticles have high biocompatibility in a wide dose range and
39
40 98 remained longer in the lungs with low systemic exposure²⁴. Thus encapsulation of apigenin
41
42 99 into albumin nanoparticles would enhance its solubility and distribution in the lung. However,
43
44 100 the formulation of dry powders with optimal aerodynamic properties for pulmonary drug
45
46 101 delivery is challenging. Spray drying is a technique for manufacturing respirable dry powders
47
48 102 in one step. During the process, the liquid phase is atomized into droplets that dry rapidly in
49
50 103 the drying chamber due to the compressed air. The process conditions like heat, flow rate,
51
52 104 aspiration rate and pump rate also determine the quality of the product. The thermal
53
54
55
56
57
58
59
60

1
2
3 105 degradation caused by overheating can be avoided by the rapid evaporation of the solvent²⁷.
4
5 106 Hence, it is suitable for drying colloidal systems resulting in uniform particle morphology.
6
7 107 Nanoparticle delivery systems targeted to the lungs offer several advantages such as sustained
8
9 108 release, increased local drug concentration and targeted site of action²⁸. Moreover, improved
10
11 109 drug solubility, uniform dose distribution and fewer side effects can be achieved, compared to
12
13 110 conventional dry powders. In general, respirable nanoparticles are embedded in microparticles
14
15 111 in aerodynamic size range²⁶.

16
17
18 112 The aim of this work was to develop a novel dry powder formulation against ALI
19
20 113 caused by oxidative stress. The prepared albumin nanoparticles were characterized in terms of
21
22 114 size, zeta potential and drug loading, additionally the fluorescence properties were
23
24 115 investigated. Following this, the nanoparticles were spray dried with two types of excipients,
25
26 116 namely a traditional lactose monohydrate and a novel amino acid, L-leucine. *In vitro* aerosol
27
28 117 deposition patterns were determined in comparison to excipient-free formulation using a next
29
30 118 generation impactor (NGI) and dissolution test was performed in simulated lung fluid by
31
32 119 using Franz cell apparatus. Laser diffraction particle sizing, morphology and residual moisture
33
34 120 content were measured along with the antioxidant activity.

35 36 37 38 121 **2. MATERIALS AND METHODS**

39 40 122 **MATERIALS**

41
42
43 123 Apigenin (Api) was purchased from (purity > 99%) Hangzhou Dadyangchem Co., Ltd.
44
45 124 (China). Bovine serum albumin powder (BSA, purity \geq 98%), L-leucine, analytical grade
46
47 125 chloroform, acetonitrile and trifluoroacetic acid (TFA) were obtained from Sigma Aldrich
48
49 126 Ltd. (Dorset, UK). Lactohale[®] LH 230 was supplied by Friesland Foods Domo (Amersfoort,
50
51 127 The Netherlands). 2,2-Diphenyl-1-picrylhydrazyl (DPPH[·]) free radical was purchased from
52
53 128 Sigma-Aldrich (Darmstadt, Germany). For the solubility and drug release study, PBS buffer
54
55 129 was purchased (Sigma Aldrich Ltd., Dorset, UK) and simulated lung fluid modified with
56
57
58
59
60

1
2
3 130 0.02% (w/v) (mSLF) was prepared. All of the materials for the mSLF were purchased from
4
5 131 Sigma Aldrich Ltd. (Dorset, UK).
6
7

8 132 **METHODS**

9 10 133 **2.1. Preparation of BSA-NPs**

11
12
13 134 BSA nanoparticles were prepared using a nanoparticle albumin bound technology with
14
15 135 minor modifications²⁹. Briefly, 1000 mg of BSA was dissolved in 50 ml of distilled water
16
17 136 saturated with chloroform. Separately, 100 mg of Api was dissolved in 3 ml of chloroform
18
19 137 saturated with water and ultrasonicated for 10 minutes. These two solutions were mixed and
20
21 138 ultrasonicated for 20 minutes with a probe-type sonicator (MSE Soniprep 150 Ultrasonic
22
23 139 Processor, MSE Ltd., London, UK) on ice. After homogenization, the chloroform was
24
25 140 evaporated by rotary evaporator (Rotavapor[®] R-10, BÜCHI Labortechnik AG, Flawil,
26
27 141 Switzerland) at 25°C for 15 minutes. The obtained nanoparticles were filtered through filter
28
29 142 paper (0.45µm, Ficher Scientific Ltd., Loughborough, UK) and further spray dried.
30
31

32 143 **2.2. Characterization of BSA-Api-NPs**

33 144 **2.2.1. Particle size and zeta potential analysis**

34
35
36
37 145 The average particle size and polydispersity index (PDI) were determined by dynamic
38
39 146 light scattering (DLS) using Zetasizer Nano ZS instrument (Malvern Instruments Ltd.,
40
41 147 Worcestershire, UK). Zeta potential of the particles was quantified with laser doppler
42
43 148 velocimetry (LDV) using the same instrument. All measurements were performed in triplicate
44
45 149 (n=3) at 25 °C and presented as mean ± standard deviation (SD).
46
47

48 150 **2.2.2. Determination of drug loading and encapsulation efficiency**

49
50 151 To determine the amount of Api, 1 ml sample from the BSA-Api formulation was
51
52 152 withdrawn and the apigenin content was determined in mg/ml by adding 5 ml of dimethyl
53
54 153 sulfoxide and methanol (DMSO:MeOH, 50:50% v/v) and sonicated for 10 minutes. The exact
55
56 154 concentrations were determined after filtration (0.22 µm) by HPLC 1260 (Agilent
57
58
59
60

Technologies Inc., Santa Clara, USA) using reverse-phase C₁₈ column (Phenomenex[®], 250x4.6 mm, 4µm) as the stationary phase. The temperature was set to 25 °C. The mobile phase consisted of 40% acetonitrile and 60% water containing 0.1% (v/v) TFA. The system was run isocratically at the flow rate of 1.2 ml/min and the Api was detected at 340 nm (t_R = 8.3). The injection volume was set to 10 µl. A calibration curve was conducted by diluting stock solution (0.1 mg/ml) with R² value of 0.999.

The drug loading efficiency (DL, %) and encapsulation efficiency (EE, %) were calculated according to the equations (Eq. 1. and 2.), comparing the encapsulated Api content (mg/ml, W_{encapsulated}) to total nanoparticle system which means the weighted amount of BSA and Api together (mg/ml, W_{total}) and the amount of Api (mg/ml, W_{theoretical}) used in the formulations.

$$DL (\%) = \frac{W_{encapsulated}}{W_{total}} \times 100 \quad \text{Eq.1.}$$

$$EE (\%) = \frac{W_{encapsulated}}{W_{theoretical}} \times 100 \quad \text{Eq.2.}$$

2.2.3. Fluorescence spectroscopy

The fluorescence emission spectra of BSA and BSA-Api-NPs were measured with Jobin Yvon-Horiba Fluoromax-3 (Paris, France) spectrofluorometer. The samples which contained the nanoparticles were diluted 10 times and the fluorescence emission spectra were recorded between 300 and 450 nm at 25 °C where the excitation wavelength was set to 285 nm. The data collection frequency was 0.5 nm and the integration time was 0.2 s. The excitation slit was set at a bandpass width of 2 nm and the emission slit at 5 nm. Each spectrum was recorded three times and the mean values were calculated automatically. The SPSEV V3.14 software (© Csaba Bagyinka, Institute of Biophysics, Biological Research Center of the Hungarian Academy of Sciences, Szeged, Hungary) was used for baseline correction, for five point linear smoothing and for the correction to the wavelength-dependent

179 sensitivity changes of the spectrofluorometer. The subtraction of the Raman band at 390 nm
180 was performed.

181 To obtain the three-dimensional projections and contour maps of fluorescence spectra
182 of the samples, the fluorescence emission were recorded from 265 to 450 nm using different
183 excitation wavelengths from 250 to 310 nm with 10 nm-steps with the same instrument
184 mentioned above. All emission scan ranges were set to start at least 15 nm away from the
185 corresponding excitation wavelengths. Other settings were similar as described above. Each
186 spectrum was recorded three times and the mean values were calculated automatically. The
187 three-dimensional fluorescence spectra were visualized with the software SURFER Version
188 10 (Golden Software, Inc., Colorado, USA). Spectra were combined together into a three
189 dimensional surface data set with axes of excitation and emission wavelengths and
190 fluorescence intensity. Data were also converted into two dimensional contour maps.

191 **2.3. Spray drying of BSA-Api-NPs**

192 Spray drying of the BSA-Api formulations without excipient and in the presence of
193 lactose monohydrate (50%, w/w) and L-leucine (9%, w/w) were carried out in a Büchi 290
194 Mini Spray Dryer (BÜCHI Labortechnik AG, Flawil, Switzerland). The concentration of the
195 excipients were with respect to the mass of the nanoparticles before spray drying. The
196 following operating conditions were used based on pilot experiments: inlet temperature 120
197 °C, approximate outlet temperature 65-70 °C, the drying airflow 600 L/h, aspiration rate
198 100% (35 m³/h), the nozzle diameter was a 0.1 mm and the liquid feed rate was set to 5
199 ml/min. Each preparation were carried out in triplicate. Following spray drying, the powders
200 were collected from the lower part of the cyclone and the collecting vessel, stored in tightly
201 sealed glass vials under vacuum at room temperature.

202 **2.4. Characterization of spray-dried BSA-Api-NPs**

203 **2.4.1. Determination of residual moisture**

1
2
3 204 The moisture content of the spray-dried powders was measured by using Karl Fischer
4
5 205 titration (Metrohm 758 KFD Titirino, Metrohm AG, Lichtenstein, Switzerland). For that
6
7 206 purpose approx. 100 mg of the product was analysed and the instrument was previously
8
9
10 207 calibrated with 10 μ l distilled water. The evaluation was conducted in triplicate and the
11
12 208 standard deviation calculated.

14 209 **2.4.2. Fourier-Transform Infrared Spectroscopy (FT-IR)**

16 210 FT-IR spectra of BSA-API spray-dried samples were evaluated using a PerkinElmer
17
18 211 Spectrum 100 FT-IR spectrometer equipped with Universal ATR (Attenuated Total
19
20 212 Reflectance) accessory (PerkinElmer Inc., Waltham, USA). Approximately 2 mg of the solid
21
22 213 samples were placed between the plate and the probe. The spectra were recorded with 3 scans,
23
24
25 214 in the frequency range between 4000-600 cm^{-1} and with a resolution of 4 cm^{-1} at room
26
27 215 temperature. The data were analyzed using the PerkinElmer Spectrum Express software.

29 216 **2.4.3. X-ray powder diffraction (XRPD)**

31 217 XRPD diffractograms were obtained using an X-ray diffractometer (MiniFlex600
32
33 218 Rigaku Corporation, Tokyo, Japan). The analyses were performed at room temperature and
34
35 219 the samples were scanned from 2° to 40° 2 θ using a scanning speed of 2°/min with a step size
36
37 220 of 0.05°.

40 221 **2.4.4. Differential scanning calorimetry (DSC) analysis**

42 222 The spray-dried formulations were characterized by DSC (DSC Q2000 module; TA
43
44 223 Instruments, New Castle, UK) which was calibrated using indium. Samples (3-5 mg) were
45
46 224 weighed accurately and analyzed in sealed and pierced aluminium hermetic pans (TA
47
48 225 Instruments). The pans were equilibrated at 25 °C and then heated at a rate of 10 °C/min in a
49
50 226 range of 50–400 °C.

54 227 **2.4.5. Aerosol particle size analysis and redispersibility in water**

1
2
3 228 The particle size analysis was conducted by using a Sympatec HELOS laser
4
5 229 diffractometer (Sympatec GmbH System-Partikel-Technik, Clausthal-Zellerfeld, Germany).

6
7 230 The powders were dispersed by compressed air (4-5 bar) into the measuring zone of the laser
8
9 231 beam. The optical lens (0.45–87.5 μm size range) focused onto the detector to collect the
10
11 232 diffracted light for calculation of size distribution. The values of 10th (D_{10}), 50th (D_{50}) and
12
13 233 90th (D_{90}) of the cumulative particle size distribution are generated. Samples were measured
14
15 234 in triplicate.

16
17
18 235 The particle size was also determined after spray drying. 5 mg dry powder of each
19
20 236 formulation could be easily redispersed in 5 ml distilled water and the particle size was
21
22 237 determined without any further dilution by the above mentioned Zetasizer Nano ZS
23
24 238 instrument (Malvern Instruments Ltd., Worcestershire, UK).

25 26 27 239 **2.4.6. Solubility and Drug release studies of BSA-Api formulations**

28
29 240 The solubility of BSA-Api formulations were determined in PBS buffer (pH 7.4) and
30
31 241 in modified simulated lung fluid (mSLF, pH 7.4) which contained 0.02% (w/v) DPPC was
32
33 242 prepared according to Son and McConville³⁰. 50 mg of samples of spray dried powders were
34
35 243 added to 100 mL solvent and shaken (150 rpm) for 2 h at 37 °C. At predetermined time points
36
37 244 1 mL of samples were taken from each dissolution media and replaced with the same volume
38
39 245 of fresh medium. All of the samples were diluted with 1 ml methanol and filtered with
40
41 246 Amicon[®] Ultra Centrifugal filters (30K, Merck Millipore, Merck KGaA, Germany) prior to
42
43 247 the injection and the amount of apigenin was determined by HPLC-UV method.

44
45
46 248 The *in vitro* drug release study of the three formulations were conducted with Franz cell
47
48 249 apparatus. The mSLF was used as dissolution media and 0.45 μm cellulose acetate membrane
49
50 250 filter (Sartorius AG, Goettingen, Germany) was applied. Briefly, an accurately weighed
51
52 251 amount (10 mg) of spray dried nanoparticles of each formulations were scattered onto the
53
54 252 membrane which was previously wetted with the dissolution media for 1 hour. 1 ml of
55
56
57
58
59
60

1
2
3 253 samples were withdrawn at various time intervals for 5 hours and replaced with fresh
4
5 254 dissolution medium. After the measurement, membrane was rinsed with 2 ml of MeOH and
6
7 255 the drug content of the possibly remained powders was determined. The sample preparation
8
9
10 256 and the measurement was the same as mentioned above. The cumulative amount of apigenin
11
12 257 release over the time was plotted for each formulations. All measurements were performed in
13
14 258 triplicate.

16 259 **2.4.7. Aerosol delivery of BSA-API formulations**

18
19 260 *In vitro* aerodynamic performance of BSA-API formulations was assessed using the
20
21 261 next generation impactor (NGI; Copley Scientific Ltd., Nottingham, UK), connected
22
23 262 sequentially to a low capacity pump via the critical flow controller (Model LCP5; Copley
24
25 263 Scientific Ltd., Nottingham, UK). During the measurement the pump was operated at air flow
26
27 264 rate of 60 L/min for 4 s. The 3x10 mg powder aliquots from each formulation were loaded
28
29 265 manually into gelatine capsules (size 3) and placed into the inhaler device (Cyclohaler[®],
30
31 266 Pharmachemie, London, UK) which was connected to the NGI via an airtight rubber adaptor
32
33 267 and a stainless steel USP throat. The NGI stages were assembled with an induction port, a
34
35 268 pre-separator and a filter was placed in the final stage. Prior to the impaction, the collection
36
37 269 plates were uniformly coated with 1 ml of 1% silicone oil in N-hexane solution and allowed
38
39 270 to dry leaving a thin film of silicone oil on the plate surface in order to prevent the re-
40
41 271 entrainment of the particles and the pre-separator was filled with 15 ml DMSO:MeOH
42
43 272 (50:50%, v/v) mixture. After the deposition of the powders in the NGI, the amount of each
44
45 273 formulation was cumulatively collected onto silicone-coated plates for each of the stages. The
46
47 274 inhaler, mouth piece, induction port, pre-separator and the collection plates were rinsed with
48
49 275 DMSO:MeOH (50:50%, v/v) mixture, collected in volumetric flasks (10 or 25 ml) and made
50
51 276 up to volume. The samples were determined by using HPLC method as described previously.
52
53
54 277 To characterize the aerosol performance the following parameters were calculated based on
55
56
57
58
59
60

1
2
3 278 the drug mass of each fraction: emitted dose (ED, %): the percentage of the entire dose
4
5 279 depositing from the mouthpiece of the inhaler device and recovered dose (RD, %): the total
6
7 280 recovered drug mass. The fine particle fraction (FPF, $<4.46 \mu\text{m}$) is defined as the percentage
8
9
10 281 of the emitted dose which deposited from the Stage 2-7 and the micro orifice-collector
11
12 282 (MOC). The mass median aerodynamic diameter (MMAD) and geometric standard deviation
13
14 283 (GSD) were calculated from the inverse of the standard normal cumulative mass distribution
15
16 284 against the natural logarithm of the effective cut-off diameter of the respective stages. All
17
18 285 measurements were carried out in triplicate.

20 286 **2.4.8. Particle morphology**

21
22
23 287 Morphology of Api powder and spray-dried nanoparticles was examined using
24
25 288 scanning electron microscopy (SEM) analysis. The dry powder of the formulations was
26
27 289 placed on the sample holder using double adhesive tape and gold coating ($\sim 20 \text{ nm}$ thickness)
28
29 290 was applied. Examinations were performed by FEI InspectTM S50 (Hillsboro, Oregon, USA)
30
31 291 scanning electron microscope at 20.00 kV accelerating voltage. Original magnifications were
32
33 292 8000x, 10,000x and 20,000 x with accuracy of $\pm 2\%$.

34 293 **2.5. Antioxidant activity**

35
36
37 294 The antioxidant activities of the prepared spray-dried formulations were compared to
38
39 295 the pure Api in order to investigate the effectiveness of the formulation. The free radical
40
41 296 scavenging activity was measured by using DPPH[•] method as described previously³¹ with
42
43 297 slight modifications. Methanolic stock solution of 0.1 mM DPPH[•] reagent was freshly
44
45 298 prepared and protected from light. Standard curve was plotted between the DPPH[•]
46
47 299 concentration (0.01-0.1 mM) and absorbance, the linear relationship was calculated
48
49 300 graphically. 1 ml of MeOH was added to the BSA-Api-NPs and the concentration of Api were
50
51 301 the same in each sample for the comparability. Thereafter 2 ml of 0.06 mM DPPH[•] reagent
52
53 302 was added to the samples, vortex mixed for 10 seconds and protected from light. The
54
55
56
57
58
59
60

absorbance at 517 nm was determined with spectrophotometer (UV-Vis spectrophotometer, Metertech SP-8001, Metertech Inc., Taipei, Taiwan) in every 15 minutes until the steady state (when no further discoloration could be observed). The addition of samples resulted decrease in the absorbance of DPPH[•] due to the scavenging activity of Api. The exact concentration of the free radical was calculated using the standard curve. To calculate the inhibition of the free radical DPPH[•] the following equation (Eq.3.) was used:

$$I (\%) = \frac{A_0 - A_s}{A_0} \times 100 \quad \text{Eq.3.}$$

Where I (%) is the inhibition in percent, A_0 is the absorbance of the DPPH[•] solution and A_s is the absorbance of the sample. All measurements were carried out triplicate and the data were expressed as the mean value \pm SD.

3. RESULTS AND DISCUSSION

3.1. Characterization of BSA-Api-NPs

3.1.1. Size, zeta potential and drug content

Albumin is a natural protein that has been widely used as a macromolecular carrier for many drugs with low water solubility. Several techniques are available to prepare albumin nanoparticles including desolvation (coacervation), nab (nanoparticle albumin bound)-technology and self-assembly¹⁴. In this study the BSA-Api-NPs were prepared by using modified nab-technology with ultrasonication. The achieved mean particle size of three samples was 376 ± 7.824 nm with a polydispersity index of 0.285 ± 0.01 . The size of albumin NPs less than 500 nm could localize effectively in the lung. The PDI value indicated narrow particle size distribution and the uniformity of the nanoparticles. The zeta potential was -19.20 ± 0.818 mV. The higher the zeta potential, the more stable the formulation is, less aggregation occurs³². The EE was determined to be $82.61 \pm 4.56\%$ and the DL was $7.51 \pm 0.415\%$. Therefore these results confirmed the high encapsulation efficiency of apigenin by BSA-NPs and it can be attractive tool in encapsulation flavonoids for delivery. Similar data were found

1
2
3 328 in the literature when encapsulating flavonoids into albumin nanoparticles. Human serum
4
5 329 albumin-bound curcumin nanoparticles resulted $7.2 \pm 2.5\%$ loading efficiency³³ and
6
7 330 scutellarin-loaded bovine serum albumin nanoparticles possess 64.46% EE and 6.73% DL³⁴.

331 **3.1.2. Fluorescence spectroscopy**

332 The phenomenon of fluorescence quenching can result from various inter and
333 intramolecular interactions such as energy transfer, conformational changes, complex
334 formation (static quenching) or collisional interaction (dynamic quenching). During static
335 quenching the quencher forms a stable non-fluorescent complex with the fluorophore,
336 however, during dynamic quenching it collides with the fluorophore and facilitates non-
337 radiative transitions to the ground state³⁵. Therefore quenching of the intrinsic fluorescence of
338 the two tryptophan residues (Trp-134 and Trp-212) of BSA can offer information about the
339 changes in molecular microenvironment of these fluorophores, located in domain I and II,
340 respectively. Trp-134 residue is located close to the protein surface in a hydrophilic
341 environment, while Trp-212 is within a protein pocket which is hydrophobic (subdomain II
342 A). The Trp-214 in human serum albumin (HSA) is located similarly to Trp-212 in BSA³⁶⁻³⁸.
343 The quenching effect of Api on fluorescence intensity of serum albumins (BSA and HSA) has
344 been studied previously^{36, 39-42} but there is no data related to its behavior in a nanoparticulate
345 system. Studies have shown that the increasing concentration of Api resulted in a decrease in
346 the fluorescence emission intensity of serum albumin solutions. This was mainly attributed to
347 complex formation (static quenching), however, it could be dynamic quenching at higher Api
348 concentrations⁴². Nevertheless, all studies concluded that Api most likely binds to the sub-
349 domain IIA of Site I side with electrostatic and hydrophobic interactions, through which H-
350 bonds and non-radiative energy transfer can occur. The binding could affect the conformation
351 of Trp micro-region but the secondary structure of serum albumin is not altered^{36, 39, 41}.

1
2
3 352 However, the pH and ionic concentrations (e.g. NaCl) can affect the fluorescence quenching
4
5 353 on the binding parameters of apigenin to BSA⁴³.
6

7 354 **Figure 2** demonstrates the fluorescence emission spectra of BSA solution, BSA-NPs
8
9 355 and BSA-Api-NPs. The fluorescence intensity of BSA-NPs decreased slightly compared to
10
11 356 BSA solution with no obvious shift of the maximum position at 350 nm. It was probably due
12
13 357 to the conformational changes of the protein. The significantly lower emission intensity of
14
15 358 BSA-Api-NPs indicates that Api could quench the fluorescence of BSA which is also
16
17 359 reflected on the 3D projections (**Figure 3**). All of these findings indicate that Api binds to the
18
19 360 Trp region (Trp-212, subdomain II A) but the spectral maximum was not affected therefore
20
21 361 hydrophobicity and polarity of the fluorophore residues are not altered. It was concluded that
22
23 362 Api can be bound to the Trp region of serum albumin nanoparticles similarly to the solutions.
24
25

26 363 **3.2. Characterization of spray-dried BSA-Api-NPs**

27 364 **3.2.1. Determination of residual moisture**

28
29 365 Moisture content is mainly influenced by the spray drying conditions. Increased heat
30
31 366 energy availability provided by regulating inlet air temperature and aspirator capacity allows
32
33 367 more efficient drying, thus resulting in the lower moisture content demonstrated. However,
34
35 368 degradation of heat sensitive materials such as proteins may occur; therefore inlet air
36
37 369 temperature should be kept below 120 °C⁴⁴. The water content is also affected by the type of
38
39 370 excipients and the ratio with the nanoparticles⁴⁵. Moisture content is an important factor that
40
41 371 can significantly influence the aerodynamic properties of aerosols. It can change the surface
42
43 372 of particles, promote aggregation and influence the crystallinity of the spray-dried samples⁴⁴.
44
45 373 In this study, the residual water content was determined by using Karl Fisher titration. All
46
47 374 formulations had relatively low moisture content which followed the rank order of L-leucine
48
49 375 (4.11 ± 0.21%, w/w) < excipient-free (4.55 ± 0.49%, w/w) < lactose (5.8 ± 0.36%, w/w)
50
51 376 containing products. These results demonstrate that the optimized outlet air temperature
52
53
54
55
56
57
58
59
60

1
2
3 377 (around 65 °C) was suitable for serum albumin. The L-leucine containing formulation had the
4
5 378 lowest water content due to the low hygroscopic behavior of this amino acid^{46, 47}. The low
6
7 379 moisture content can potentially improve the flowability and consequently enhance lung
8
9
10 380 deposition due to reduced aggregation as expected. Storage conditions are also important, e.g.
11
12 381 the spray-dried amorphous lactose particles could transform into crystals easily in humidity
13
14 382 above 30%⁴⁸.

16 383 3.2.2. Fourier-Transform Infrared Spectroscopy (FT-IR)

18 384 FTIR analysis allows a quick and efficient identification of the compounds and by
19
20 385 their functional groups and bond vibrations. In the spectrum of raw Api, the following
21
22 386 characteristic regions were observed: 2710-2580 cm⁻¹ O-H bond, 1730-1680 cm⁻¹ C=O stretch
23
24 387 and 1450-1380 cm⁻¹ C-H bend. A broad peak observed at 3300 cm⁻¹ can be attributed to O-H
25
26 388 stretching and those bands at 1600-1400 cm⁻¹ (C-C stretch in ring) and 900-675 cm⁻¹ (C-H
27
28 389 ‘oop’) can be assigned to the aromatic group (**Figure 4 A**). In the spectrum of BSA protein,
29
30 390 the amide I band at 1635 cm⁻¹ (mainly C=O stretch) and amide II band at 1530–1500 cm⁻¹ (C–
31
32 391 N stretching and N–H bend) can be seen. The medium broad peak at 3276 cm⁻¹ corresponds to
33
34 392 bonded N-H stretch of amide and a smaller band at 1057 cm⁻¹ is the C-N stretch of aliphatic
35
36 393 amine. In the spectra of the excipients-free formulation, the characteristic amide bands of
37
38 394 BSA can be seen and peak at 830 cm⁻¹ indicating the presence of Api (aromatic) which is an
39
40 395 indirect confirmation of Api encapsulation on BSA-NPs. Conformational changes can be
41
42 396 suggested due to the lack of the peak of aliphatic amine.

47 397 The spectra of raw Api, BSA, lactose and lactose containing product are displayed on **Figure**
48
49 398 **4 B**. In the spectra of lactose there is also a broad band around 3300 cm⁻¹ indicating the
50
51 399 stretching vibration of hydroxyl group. A weak band at 1654 cm⁻¹ is the bending vibration of
52
53 400 the crystalline water and peaks at 1200-1070 cm⁻¹ demonstrate the stretching vibration of C-
54
55 401 O-C in the glucose and galactose. The spectrum of amorphous lactose has the less number and
56
57
58
59
60

1
2
3 402 defined peaks and therefore it could be distinguished from the crystalline spectrum⁴⁹. The
4
5 403 characteristic broad band at 3300 cm⁻¹ in the spectrum of spray-dried product could originate
6
7 404 from the residual water content that is further supported by the Karl Fischer titration data
8
9 405 (lactose containing product had the highest water content). Similarly to the spectrum of
10
11 406 excipients-free formulation, the amide bands of BSA and a small peak of Api could be
12
13 407 observed. The peaks at 1200-1070 cm⁻¹ demonstrate the lactose content and the amorphous
14
15 408 state could be assumed.

16
17
18 409 Functional groups of L-leucine lead to its characteristic spectrum (**Figure 4 C**). The strong
19
20 410 band in the region of 2970-2910 cm⁻¹ can be accounted for the aliphatic C-H stretching. The
21
22 411 bonded N-H stretch is present in the region of 2600-2450 cm⁻¹. The NH₂ bending and the C-
23
24 412 N skeletal vibration appear in the regions of 1595-1550 cm⁻¹ and 1250-1020 cm⁻¹ ⁵⁰. The
25
26 413 presence of BSA characteristic peaks on the spray-dried formulation could be mainly
27
28 414 observed with and a small peak of Api but the major characteristic peaks of L-leucine are
29
30 415 obscured.

34 416 **3.2.3. X-ray powder diffraction (XRPD)**

35
36 417 XRPD is considered to be the most accurate method to study crystalline structure⁵¹.
37
38 418 The combined XRPD diffractograms of Api and spray-dried formulations are presented in
39
40 419 **Figure 5**. The characteristic narrow diffraction peaks of Api are due to the crystalline state of
41
42 420 the commercially available material. In comparison, broad diffuse peaks could be observed in
43
44 421 the diffractograms of the spray-dried formulations suggesting the amorphous state of BSA-
45
46 422 Api-NPs. The observed XRD patterns of spray-dried L-leucine and lactose were consistent
47
48 423 with literature^{48, 52, 53}.

51 424 **3.2.4. Differential scanning calorimetry analysis (DSC)**

52
53
54 425 The DSC curves of raw Api, excipients, physical mixtures and spray-dried
55
56 426 formulations were studied to examine crystallinity. As seen in **Figure 6**, there is only one
57
58
59
60

1
2
3 427 sharp endothermic peak at 360 °C indicating the melting point of raw Api; no impurities were
4
5 428 observed. Drug free albumin exhibited two broad peaks with onset values of 220 °C and 310
6
7 429 °C. The evaporation of residual water occurred at 50-120 °C. The melting point of Api on the
8
9 430 thermograms of raw material and physical mixtures corresponds to the crystalline habitus. In
10
11 431 the thermograms of physical mixtures on **Figure 6 B** the endothermic peak at 140 °C
12
13 432 indicating the crystalline lactose⁵⁴ and the sublimation of L-leucine crystals occurred at 200-
14
15 433 230 °C (**Figure 6 C**)⁵⁵. However, in each spray-dried formulation the absence of endotherms
16
17 434 confirms the loss of crystallinity. No peak could be observed around 360 °C indicating that
18
19 435 Api is in amorphous state due to the spray drying process which is in agreement with the
20
21 436 XRPD diffractograms. The amorphous form generated may result higher solubility of the
22
23 437 powders and dissolution of apigenin in lung fluids.
24
25
26

27 438 **3.2.5. Aerosol particle size analysis and redispersibility in water**

28
29 439 Dry powder formulations of BSA-Api-NPs were prepared with the aim of studying the
30
31 440 influence of excipients on the particle size and aerodynamic behavior. The deposition of
32
33 441 aerosols is significantly affected by particle size which should be small enough to pass
34
35 442 through the upper airways and large enough to avoid exhalation⁵⁶. Gravitational
36
37 443 sedimentation is the main driving force for deposition of a nanoparticulate system in the lung
38
39 444 due to the formation of aggregates in the micrometer size range. Particle geometry and surface
40
41 445 properties also play a significant role in reaching the bronchioles^{22,32}. It is well known that
42
43 446 particles can be deposited efficiently deeper in the lung if their aerodynamic diameter is in the
44
45 447 range of 1-5 µm and only those with 1-3 µm can reach the respiratory zone⁵⁷. Particles, larger
46
47 448 than 5 µm tend to deposit in the oropharynx and the mucociliary clearance plays a role in
48
49 449 clearing the particles towards the pharynx. However, very small particles, less than 1 µm are
50
51 450 usually exhaled because of the low inertia^{58,59}. Mucociliary clearance is the part of the natural
52
53 451 defense mechanism of the lung as well as the phagocytosis of macrophages in the alveolar
54
55
56
57
58
59
60

1
2
3 452 region. The aerosol particle size was determined by Sympatec HELOS laser diffractometer
4
5 453 (**Table 1**). The excipient-free and lactose containing products have similar sizes while spray
6
7 454 drying with L-leucine produced the smallest particles ($D_{50} = 2.473 \mu\text{m}$). In all cases, the
8
9
10 455 particle size could ensure the highest probability of delivery of apigenin into the respiratory
11
12 456 zone.

13
14 457 Following the re-dispersion of spray powders formulations in distilled water, the size of the
15
16 458 particles was preserved in the nanometer size range: without excipient ($358.9 \pm 5.3 \text{ nm}$, PDI:
17
18 459 0.315 ± 0.013), lactose ($366.1 \pm 4.8 \text{ nm}$, PDI: 0.382 ± 0.014) and L-leucine (343.7 ± 2.9 , PDI:
19
20 460 0.316 ± 0.011) containing products. The spray drying has no significant effect on the average
21
22 461 size of the particles suggesting the deposition of apigenin containing nanoparticles in the lung
23
24 462 fluid. Moreover, the excipients did not affect adversely the particle size.

25 26 27 463 **3.2.6. Solubility and Drug release studies of BSA-Api formulations**

28
29 464 The solubility of apigenin in nanoparticles was investigated in PBS buffer and mSLF
30
31 465 (**Figure 7 A**). The results showed that the solubility was slightly increased in mSLF media
32
33 466 (82-98% within 5 minutes), however, it was high in PBS buffer as well (79-95% within 5
34
35 467 minutes). These data indicated that the solubility of apigenin could be highly enhanced by
36
37 468 BSA nanoparticles in aqueous medium. Nevertheless, the dispersibility enhancers could play
38
39 469 a role in the solubility. In case of excipient free formulation, 91% of the encapsulated
40
41 470 apigenin was dissolved in mSLF within 5 minutes. Formulation prepared with lactose
42
43 471 increased the solubility rate up to 98%, however, it was slower (82%) when using L-leucine
44
45 472 and completed within 2 hours. These results could be attributed to the solubility of the
46
47 473 excipients themselves: lactose has very good water solubility, but L-leucine possess a low
48
49 474 solubility in water⁶⁰.

50
51
52 475 The apigenin release from the spray dried BSA-Api NPs was investigated with Franz
53
54 476 cell apparatus. It is a well known device for the dissolution of semisolid dosage forms and
55
56
57
58
59
60

1
2
3 477 approved by the USP (United States Pharmacopeia). However, there is no standardized
4
5 478 method for inhaled powders, Franz cell could be one of the alternative choices due to
6
7 479 simulating the diffusion controlled air-liquid interface of the lung. On the contrary, it has
8
9 480 some limitations such as small air bubbles under the contact area of membrane to dissolution
10
11 481 medium, wide range of standard deviation or the recovery usually around maximum 90%⁶¹.
12
13 482 Based on the solubility measurements, mSLF was applied. The cumulative dissolution curves
14
15 483 of the prepared formulations are shown in **Figure 7 B**. As expected, the dissolution was
16
17 484 affected by the co-spray dried excipients. Lactose containing product resulted the fastest and
18
19 485 highest apigenin release due to the excellent water solubility. This enhancement of the
20
21 486 dissolution is supported by previously published data⁶². In contrast, the dissolution rate was
22
23 487 decreased when L-leucine was applied. The coating layer of L-leucine slowed down the
24
25 488 dissolution of apigenin which could be well observed in the dissolution curve. The low water
26
27 489 solubility of L-leucine is able to hinder the dissolution of the drug which was published
28
29 490 previously⁶⁰. These results suggest that the excipients play an important role in the solubility
30
31 491 and the dissolution as well.
32
33
34
35

36 492 **3.2.7. Aerosol delivery of BSA-Api formulations**

37
38 493 Particles can be taken up by alveolar macrophages which influences the therapeutic
39
40 494 outcome. Those nanoparticles which are soluble and above 200 nm are able to escape from
41
42 495 the macrophages therefore exhibit sustained therapeutic effect⁶³. The lung deposition and
43
44 496 therefore the efficacy of the inhaled therapeutics are governed by their aerosol properties⁵⁶.
45
46 497 Manufacturing respirable nanoparticles could be produced by aggregation in the favorable
47
48 498 size range or their incorporation into microparticles (1-5 μm)²⁶. Lactose monohydrate is a
49
50 499 well-known, traditional carrier for improving the performance of inhaled products; however,
51
52 500 it is influenced by physicochemical properties and interaction with the active ingredient^{64, 65}.
53
54 501 It is the only FDA approved carrier and has also been shown to be a potential excipient for
55
56
57
58
59
60

1
2
3 502 protein encapsulation^{27, 65}. Recently, novel materials such as specific amino acids have been
4
5 503 developed for pulmonary formulations²⁶ and L-leucine is one of the most effective
6
7 504 dispersibility enhancer among them⁴⁷. Previous studies proved that 5% (w/w) L-leucine
8
9 505 improved the aerosol performance of raw naringin⁶⁶ and inclusion up to 15% (w/w) L-leucine
10
11 506 resulted higher ED and FPF of powder formulation of gentamicin⁴⁶.

12
13
14 507 In this study *in vitro* aerosol properties of three different dry powders formulations
15
16 508 were evaluated using the NGI which is regarded as an optimal instrument for analysis of
17
18 509 aerodynamic behavior of aerosol formulations for pulmonary drug delivery⁶⁷ according to
19
20 510 European and US Pharmacopeias. The obtained data and deposition pattern are presented in
21
22 511 **Table 2** and in **Figure 8**. It can be seen that more than 90% of apigenin could be recovered
23
24 512 from the NGI which is in the acceptable pharmacopeia range (75-125%). The ED ranged
25
26 513 between 91-96% indicating good flowability and high dispersibility of the powders. L-leucine
27
28 514 containing formulation had the highest ED as it could improve significantly the flowability of
29
30 515 the powders^{47, 53}. **Figure 8** shows the amount of Api deposited on the throat, device and
31
32 516 stages 1-7 expressed as a percentage of the total amount of recovered powder. All formulation
33
34 517 exhibited increased deposition in Stage 2 - 4 indicating enhanced drug delivery to the alveolar
35
36 518 regions. As expected, improved aerosol performance and deposition (Stage 3 and 4) could be
37
38 519 observed when L-leucine was used as an excipient. The FPF is one of the key parameters in
39
40 520 aerosol delivery and should be as high as possible⁶⁸. In this study, the FPF values ranged
41
42 521 between 58-66%, suggesting that the particles could be delivered into the peripheral regions.
43
44 522 Spray drying of nanoparticles in the presence of L-leucine resulted higher FPF value (66%)
45
46 523 due to the improved surface properties and morphology of the particles⁶⁵. In general, MMAD
47
48 524 values < 5 μm are for pulmonary lung delivery and between 2-3 μm are optimal for deep lung
49
50 525 deposition⁵⁶. In each case, the calculated mass median aerodynamic diameter (MMAD) data
51
52 526 were in agreement with the physical diameter size of the particles measured by laser
53
54
55
56
57
58
59
60

1
2
3 527 diffractometer. The data obtained ($< 5 \mu\text{m}$) support good dispersibility of the particles into the
4
5 528 lower airways and the deep lung. Therefore local delivery to the alveoli could be assured by
6
7 529 both excipient-free and lactose formulations generated (MMAD $3.2 \mu\text{m}$ and $3.1 \mu\text{m}$).
8
9 530 Moreover, formulation with L-leucine (MMAD $2.1 \mu\text{m}$) would be more optimal for deep lung
10
11 531 deposition. The size distribution of an aerosol is described best by GSD⁶⁹. Based on the GSD
12
13 532 data obtained, the L-leucine containing formulation had the narrowest size distribution (1.8
14
15 533 μm) but that of the others was also in the acceptable range ($< 3 \mu\text{m}$).
16
17 534 The overall values demonstrate that the particles of each dry powder nanoparticle formulation
18
19 535 are in the favorable aerodynamic size range, possess good dispersibility properties and
20
21 536 particle deposition. Therefore BSA-NPs is an attractive delivery system for pulmonary drug
22
23 537 delivery. We demonstrated that L-leucine improved better the aerosolization properties of
24
25 538 BSA-Api-NPs than lactose monohydrate. Therefore it can be concluded that the use of
26
27 539 excipients influence the aerosol performance of nanoparticles.
28
29
30
31

32 **3.2.8. Particle morphology**

33
34 541 SEM analysis was conducted to investigate the morphology of the powders (**Figure 9**
35
36 542 **A and B**). It is well known that the morphology of the particles is strongly affected by the
37
38 543 solubility of the components and the nature of the excipients^{46,47}. The commercially available
39
40 544 Api was a crystalline powder featuring needle-shaped crystals. The excipient-free spray-dried
41
42 545 nanoparticles exhibited spherical shape and smooth or wrinkled surface. Particles of lactose
43
44 546 containing product had raisin-like surface and some of the particles were larger in accordance
45
46 547 with the laser diffraction particle size analysis. Powders prepared with L-leucine comprised
47
48 548 small and collapsed particles with strongly corrugated surface. The low aqueous solubility of
49
50 549 L-leucine leading to a shell on the surface of the droplet which interfere with the diffusion of
51
52 550 water therefore corrugated particles could form. This outcome was consistent with previous
53
54 551 observations^{46,53,70}. Corrugated surface improves the dispersibility of the dry powder
55
56
57
58
59
60

1
2
3 552 formulations and enhance respirability due to the reduced interparticulate cohesion (Van der
4
5 553 Waals forces) which is beneficial for particles intended for inhalation⁷¹.

554 **3.3. Antioxidant activity**

555 Owing to its reproducibility and comparability, the DPPH[•] assay is an established
556 method for investigating the antioxidant properties of natural compounds. Due to the H-
557 donating ability of the antioxidants, a stable reduced DPPH-H molecule can form. The
558 reaction can be seen visually and the detection can be carried out using UV-Vis
559 spectrophotometer^{72, 73}. Previous studies confirmed that Api is able to scavenge the DPPH[•]
560 free radical even in nanoscale delivery formulation^{74, 75}. In general, the scavenging activity is
561 influenced by concentration and structural features like hydrogen donating ability, position
562 and the degree of hydroxylation^{76, 77}. In order to calculate the exact concentration of
563 remaining DPPH[•] in the samples a calibration curve was plotted with $R^2=0.9999$. The time
564 required to reach the steady state was estimated to be 120 minutes, and the slow reaction
565 kinetic of Api has been reported⁷⁴. The discoloration of the deep purple DPPH[•] free radical
566 indicate the antioxidant properties of free and encapsulated Api. The inhibition of free
567 radicals by the prepared spray-dried formulations were compared to the empty BSA-NPs,
568 methanolic Api solution and “empty” nanoparticles (**Figure 10**). It can be seen that the free
569 and encapsulated Api have similar scavenging activity, moreover, the spray drying did not
570 result in the loss of scavenging activity. It has been reported that serum albumin is a
571 physiological circulating antioxidant in the body⁷⁸ which is confirmed by the inhibition
572 capacity of the empty BSA-NPs observed. Similar results were reported when encapsulating
573 rutin and keampferol⁷⁹ or quercetin¹⁷ where the antioxidant activity of the flavonoids are
574 retained by BSA. It can be concluded that the antioxidant activity of Api is preserved,
575 moreover, slightly enhanced by the BSA.

576 **4. CONCLUSION**

1
2
3 577 In this study novel apigenin containing albumin nanoparticles were prepared for
4
5 578 inhalation against lung injury caused by oxidative stress. Apigenin was recently classified as a
6
7 579 BCS II. drug with prominent antioxidant and anti-inflammatory properties in the lung. The
8
9
10 580 obtained results confirmed that incorporation of apigenin into the biocompatible albumin
11
12 581 nanoparticles resulted high encapsulation efficiency therefore it could be an attractive tool for
13
14 582 the delivery. Moreover, the spray dried nanoparticles possess good ability to re-disperse in
15
16 583 aqueous media and size of the particles was preserved in the nanometer size range. The
17
18 584 influence of dispersibility enhancers on the physicochemical properties and *in vitro*
19
20 585 pulmonary deposition were investigated and compared to the excipient-free formulation. The
21
22 586 obtained *in vitro* pulmonary depositions proved that the developed BSA-NP dry powders are
23
24 587 potentially able to carry apigenin deep in the lung, reaching the respiratory zone. The use of
25
26 588 novel excipient amino acid L-leucine resulted enhanced aerodynamic properties over the
27
28 589 traditional lactose monohydrate, indicating that the nature of the excipients and morphology
29
30 590 of the particles play a significant role in the formulation of nanoparticles for pulmonary
31
32 591 delivery. In addition, the solubility and dissolution characteristics of apigenin from
33
34 592 nanoparticles were determined in mSLF dissolution media, the co-spray dried excipients
35
36 593 played an important role. The dissolution rate was increased by the water soluble lactose and
37
38 594 decreased by L-leucine, which has low water solubility. Therefore the use of excipients should
39
40 595 be taken into consideration, may not required in case of albumin nanoparticles. We further
41
42 596 confirmed that the antioxidant activity is retained, thus the potential of albumin nanoparticles
43
44 597 as an effective pulmonary delivery system for flavonoids such as apigenin.

49 598 **ACKNOWLEDGEMENTS**

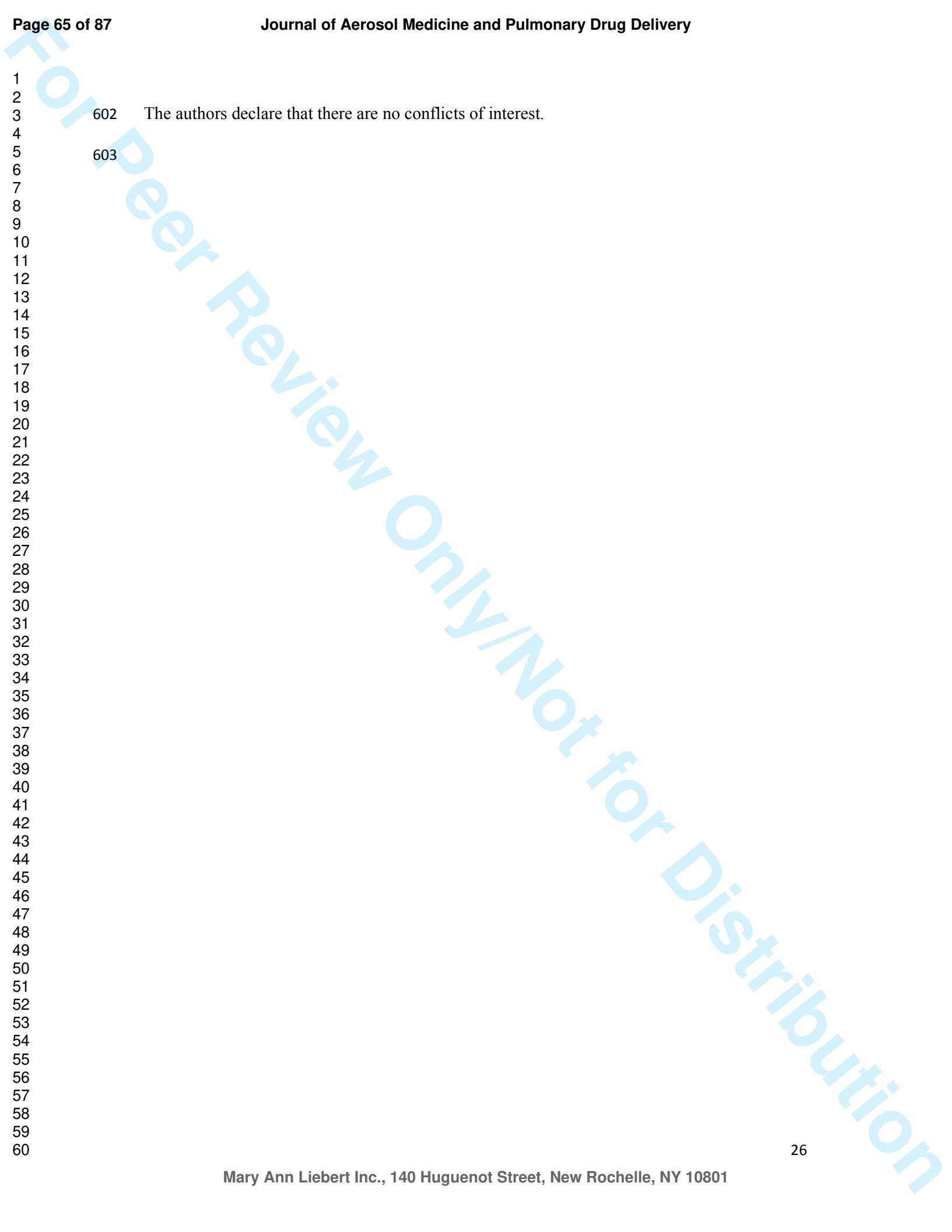
50
51
52 599 The authors gratefully acknowledge to Róbert Kovács for providing the SEM pictures at
53
54 600 Budapest University of Technology and Economics.

55 601 **Author Disclosure Statement**

1
2
3
4
5
6
7
8
9
10
11
12
13
14
15
16
17
18
19
20
21
22
23
24
25
26
27
28
29
30
31
32
33
34
35
36
37
38
39
40
41
42
43
44
45
46
47
48
49
50
51
52
53
54
55
56
57
58
59
60

602 The authors declare that there are no conflicts of interest.

603



604 **REFERENCES**

- 605 **1.** Chow C-W, Herrera Abreu MT, Suzuki T, and Downey GP. Oxidative Stress and
606 Acute Lung Injury. *Am J Respir Cell Mol Biol.* 2003;29:427-431.
- 607 **2.** Chen XW, Serag ES, Sneed KB, and Zhou SF. Herbal bioactivation, molecular targets
608 and the toxicity relevance. *Chem Biol Interact.* 2011;192:161-176.
- 609 **3.** Patel D, Shukla S, and Gupta S. Apigenin and cancer chemoprevention: progress,
610 potential and promise (review). *Int J Oncol.* 2007;30:233-245.
- 611 **4.** Kim SJ, Jeong HJ, Moon PD, Lee KM, Lee HB, Jung HJ, Jung SK, Rhee HK, Yang
612 DC, Hong SH, and Kim HM. Anti-inflammatory activity of gumiganghwaltang
613 through the inhibition of nuclear factor-kappa B activation in peritoneal macrophages.
614 *Biol Pharm Bull.* 2005;28:233-237.
- 615 **5.** Kowalski J, Samojedny A, Paul M, Pietsz G, and Wilczok T. Effect of apigenin,
616 kaempferol and resveratrol on the expression of interleukin-1beta and tumor necrosis
617 factor-alpha genes in J774.2 macrophages. *Pharmacol Rep.* 2005;57:390-394.
- 618 **6.** Lee J-H, Zhou H, Cho S, Kim Y, Lee Y, and Jeong C. Anti-inflammatory mechanisms
619 of apigenin: inhibition of cyclooxygenase-2 expression, adhesion of monocytes to
620 human umbilical vein endothelial cells, and expression of cellular adhesion molecules.
621 *Archives of Pharmacal Research.* 2007;30:1318-1327.
- 622 **7.** Chen L and Zhao WEI. Apigenin protects against bleomycin-induced lung fibrosis in
623 rats. *Exp Ther Med.* 2016;11:230-234.
- 624 **8.** Luan RL, Meng XX, and Jiang W. Protective Effects of Apigenin Against Paraquat-
625 Induced Acute Lung Injury in Mice. *Inflammation.* 2016; 39:752-758.
- 626 **9.** Basios N, Lampropoulos P, Papalois A, Lambropoulou M, Pitiakoudis MK, Kotini A,
627 Simopoulos C, and Tsaroucha AK. Apigenin Attenuates Inflammation in

- 1
2
3 628 Experimentally Induced Acute Pancreatitis-Associated Lung Injury. *J Invest Surg.*
4
5 629 2015;2:1-7.
6
7 630 **10.** Patil R, Babu RL, Naveen Kumar M, Kiran Kumar KM, Hegde S, Ramesh G, and
8
9 631 Chidananda Sharma S. Apigenin inhibits PMA-induced expression of pro-
10
11 632 inflammatory cytokines and AP-1 factors in A549 cells. *Mol Cell Biochem.*
12
13 633 2015;403:95-106.
14
15
16 634 **11.** Wang J, Liu Y-T, Xiao L, Zhu L, Wang Q, and Yan T. Anti-Inflammatory Effects of
17
18 635 Apigenin in Lipopolysaccharide-Induced Inflammation in Acute Lung Injury by
19
20 636 Suppressing COX-2 and NF- κ B Pathway. *Inflammation.* 2014;37:2085-2090.
21
22
23 637 **12.** Zhang J, Liu D, Huang Y, Gao Y, and Qian S. Biopharmaceutics classification and
24
25 638 intestinal absorption study of apigenin. *Int J Pharm.* 2012;436:311-317.
26
27 639 **13.** Ajazuddin and Saraf S. Applications of novel drug delivery system for herbal
28
29 640 formulations. *Fitoterapia.* 2010;81:680-689.
30
31 641 **14.** Elzoghby AO, Samy WM, and Elgindy NA. Albumin-based nanoparticles as potential
32
33 642 controlled release drug delivery systems. *J Control Release.* 2012;157:168-182.
34
35
36 643 **15.** Hu Y-J, Liu Y, Sun T-Q, Bai A-M, Lü J-Q, and Pi Z-B. Binding of anti-inflammatory
37
38 644 drug cromolyn sodium to bovine serum albumin. *Int J Biol Macromolec.* 2006;39:280-
39
40 645 285.
41
42
43 646 **16.** Fasano M, Curry S, Terreno E, Galliano M, Fanali G, Narciso P, Notari S, and
44
45 647 Ascenzi P. The extraordinary ligand binding properties of human serum albumin.
46
47 648 *IUBMB Life.* 2005;57:787-796.
48
49 649 **17.** Fang R, Hao R, Wu X, Li Q, Leng X, and Jing H. Bovine Serum Albumin
50
51 650 Nanoparticle Promotes the Stability of Quercetin in Simulated Intestinal Fluid. *J Agr*
52
53 651 *Food Chem.* 2011;59:6292-6298.
54
55
56
57
58
59
60

- 1
2
3 652 **18.** He X, Xiang N, Zhang J, Zhou J, Fu Y, Gong T, and Zhang Z. Encapsulation of
4
5 653 teniposide into albumin nanoparticles with greatly lowered toxicity and enhanced
6
7 654 antitumor activity. *Int J Pharm.* 2015;487:250-259.
- 8
9
10 655 **19.** Muralidharan P, Malapit M, Mallory E, Hayes Jr D, and Mansour HM. Inhalable
11
12 656 nanoparticulate powders for respiratory delivery. *Nanomedicine: NBM.* 2015;11:1189-
13
14 657 1199.
- 15
16 658 **20.** Malcolmson RJ and Embleton JK. Dry powder formulations for pulmonary delivery.
17
18 659 *Pharm Sci Technol To.* 1998;1:394-398.
- 19
20
21 660 **21.** Stegemann S, Kopp S, Borchard G, Shah VP, Senel S, Dubey R, Urbanetz N, Cittero
22
23 661 M, Schoubben A, Hippchen C, Cade D, Fuglsang A, Morais J, Borgström L, Farshi F,
24
25 662 Seyfang KH, Hermann R, van de Putte A, Klebovich I, and Hincal A. Developing and
26
27 663 advancing dry powder inhalation towards enhanced therapeutics. *Eur J Pharm Sci.*
28
29 664 2013;48:181-194.
- 30
31
32 665 **22.** Yang W, Peters JI, and Williams Iii RO. Inhaled nanoparticles—A current review. *Int*
33
34 666 *J Pharm.* 2008;356:239-247.
- 35
36 667 **23.** Geiser M. Update on macrophage clearance of inhaled micro- and nanoparticles. *J*
37
38 668 *Aerosol Med Pulm Drug Deliv.* 2010;23:207-217.
- 39
40
41 669 **24.** Woods A, Patel A, Spina D, Riffo-Vasquez Y, Babin-Morgan A, de Rosales RT,
42
43 670 Sunassee K, Clark S, Collins H, Bruce K, Dailey LA, and Forbes B. In vivo
44
45 671 biocompatibility, clearance, and biodistribution of albumin vehicles for pulmonary
46
47 672 drug delivery. *J Control Release.* 2015;210:1-9.
- 48
49
50 673 **25.** Swarbrick J. *Encyclopedia of Pharmaceutical Technology.* Informa
51
52 674 Healthcare:London; 2007; 671 - 1434.
- 53
54 675 **26.** Mansour HM, Rhee YS, and Wu X. Nanomedicine in pulmonary delivery. *Int J*
55
56 676 *Nanomedicine.* 2009;4:299-319.

- 1
2
3 677 27. Shoyele SA and Cawthorne S. Particle engineering techniques for inhaled
4
5 678 biopharmaceuticals. *Adv Drug Deliv Rev.* 2006;58:1009-1029.
6
7 679 28. Sung JC, Pulliam BL, and Edwards DA. Nanoparticles for drug delivery to the lungs.
8
9 680 *Trends Biotechnol.* 2007;25:563-570.
10
11 681 29. Desai NP, Tao C, Yang A, Louie L, Yao Z, Soon-Shiong P, and Magdassi S. Protein
12
13 682 stabilized pharmacologically active agents, methods for the preparation thereof and
14
15 683 methods for the use thereof. Google Patents, 2004. US6749868 B1
16
17 684 30. Son YJ, McConville JT. Development of a standardized dissolution test method for
18
19 685 inhaled pharmaceutical formulations. *Int J Pharm.* 2009;382:15–22.
20
21 686 31. Hatano T. KH, Yasuhara T., Okuda T. 2 new flavonoids and other constituents in
22
23 687 licorice root-their relative astringency and radical scavenging effects. *Chem Pharm*
24
25 688 *Bull.* 1988;36:2090-2097.
26
27 689 32. Paranjpe M and Muller-Goymann CC. Nanoparticle-mediated pulmonary drug
28
29 690 delivery: a review. *Int J Mol Sci.* 2014;15:5852-5873.
30
31 691 33. Kim TH, Jiang HH, Youn YS, Park CW, Tak KK, Lee S, Kim H, Jon S, Chen X, and
32
33 692 Lee KC. Preparation and characterization of water-soluble albumin-bound curcumin
34
35 693 nanoparticles with improved antitumor activity. *Int J Pharm.* 2011;403:285-291.
36
37 694 34. Wei Y, Li L, Xi Y, Qian S, Gao Y, and Zhang J. Sustained release and enhanced
38
39 695 bioavailability of injectable scutellarin-loaded bovine serum albumin nanoparticles. *Int*
40
41 696 *J Pharm.* 2014;476:142-148.
42
43 697 35. Valeur B. *Molecular fluorescence principles and applications.* Wiley-VCH:
44
45 698 Weinheim; 2002; 73-124.
46
47 699 36. Yuan J-L, lv Z, Liu Z-G, Hu Z, and Zou G-L. Study on interaction between apigenin
48
49 700 and human serum albumin by spectroscopy and molecular modeling. *J Photochem*
50
51 701 *Photobiol A.* 2007;191:104-113.
52
53
54
55
56
57
58
59
60

- 1
2
3 702 37. Naveenraj S and Anandan S. Binding of serum albumins with bioactive substances –
4
5 703 Nanoparticles to drugs. *J Photochem Photobiol C*. 2013;14:53-71.
6
7 704 38. Tayeh N, Rungassamy T, and Albani JR. Fluorescence spectral resolution of
8
9 705 tryptophan residues in bovine and human serum albumins. *J Pharm Biomed Anal*.
10
11 706 2009;50:107-116.
12
13 707 39. Zhao X-N, Liu Y, Niu L-Y, and Zhao C-P. Spectroscopic studies on the interaction of
14
15 708 bovine serum albumin with surfactants and apigenin. *Spectrochim Acta A Mol Biomol*
16
17 709 *Spectrosc*. 2012;94:357-364.
18
19 710 40. Lin C-Z, Hu M, Wu A-Z, and Zhu C-C. Investigation on the differences of four
20
21 711 flavonoids with similar structure binding to human serum albumin. *J Pharm Anal*.
22
23 712 2014;4:392-398.
24
25 713 41. Cao H, Liu Q, Shi J, Xiao J, and Xu M. Comparing the Affinities of Flavonoid
26
27 714 Isomers with Protein by Fluorescence Spectroscopy. *Anal Lett*. 2008;41:521-532.
28
29 715 42. Shang Y and Li H. Studies of the interaction between apigenin and bovine serum
30
31 716 albumin by spectroscopic methods. *Russ J Gen Chem*. 2010;80:1710-1717.
32
33 717 43. Tang L, Jia W, and Zhang D. The effects of experimental conditions of fluorescence
34
35 718 quenching on the binding parameters of apigenin to bovine serum albumin by
36
37 719 response surface methods. *Luminescence*. 2014;29:344-351.
38
39 720 44. Stahl K, Claesson M, Lilliehorn P, Linden H, and Backstrom K. The effect of process
40
41 721 variables on the degradation and physical properties of spray dried insulin intended for
42
43 722 inhalation. *Int J Pharm*. 2002;233:227-237.
44
45 723 45. Jensen DM, Cun D, Maltesen MJ, Frokjaer S, Nielsen HM, and Foged C. Spray drying
46
47 724 of siRNA-containing PLGA nanoparticles intended for inhalation. *J Control Release*.
48
49 725 2010;142:138-145.
50
51
52
53
54
55
56
57
58
59
60

- 1
2
3 726 46. Aquino RP, Prota L, Auriemma G, Santoro A, Mencherini T, Colombo G, and Russo
4
5 727 P. Dry powder inhalers of gentamicin and leucine: formulation parameters, aerosol
6
7 728 performance and in vitro toxicity on CuFi1 cells. *Int J Pharm.* 2012;426:100-107.
8
9
10 729 47. Yang X-F, Xu Y, Qu D-S, and Li H-Y. The influence of amino acids on aztreonam
11
12 730 spray-dried powders for inhalation. *Asian J Pharm Sci.* 2015;10:541-548.
13
14 731 48. Wu L, Miao X, Shan Z, Huang Y, Li L, Pan X, Yao Q, Li G, and Wu C. Studies on
15
16 732 the spray dried lactose as carrier for dry powder inhalation. *Asian J Pharm Sci.*
17
18 733 2014;9:336-341.
19
20 734 49. Listiohadi Y, Hourigan J, Sleigh R, and Steele R. Thermal analysis of amorphous
21
22 735 lactose and α -lactose monohydrate. *Dairy Sci Technol.* 2009;89:43-67.
23
24
25 736 50. Němec I and Mička Z. FTIR and FT Raman study of L-leucine addition compound
26
27 737 with nitric acid. *J Mol Struct.* 1999;482-483:23-28.
28
29
30 738 51. Newman AW and Byrn SR. Solid-state analysis of the active pharmaceutical
31
32 739 ingredient in drug products. *Drug Discov Today.* 2003;8:898-905.
33
34 740 52. Sou T, Kaminskis LM, Nguyen T-H, Carlberg R, McIntosh MP, and Morton DAV.
35
36 741 The effect of amino acid excipients on morphology and solid-state properties of multi-
37
38 742 component spray-dried formulations for pulmonary delivery of biomacromolecules.
39
40 743 *Eur J Pharm Biopharm.* 2013;83:234-243.
41
42
43 744 53. Mangal S, Meiser F, Tan G, Gengenbach T, Denman J, Rowles MR, Larson I, and
44
45 745 Morton DAV. Relationship between surface concentration of l-leucine and bulk
46
47 746 powder properties in spray dried formulations. *Eur J Pharm Biopharm.* 2015;94:160-
48
49 747 169.
50
51
52 748 54. Gombás Á, Szabó-Révész P, Kata M, Regdon G, Jr., and Erős I. Quantitative
53
54 749 Determination of Crystallinity of α -Lactose Monohydrate by DSC. *J Therm Anal*
55
56 750 *Calorim.* 2002;68:503-510.
57
58
59
60

- 1
2
3 751 **55.** Raula J, Seppälä J, Malm J, Karppinen M, and Kauppinen EI. Structure and
4
5 752 Dissolution of l-Leucine-Coated Salbutamol Sulphate Aerosol Particles. *AAPS*
6
7 753 *PharmSciTech*. 2012;13:707-712.
8
9
10 754 **56.** Yang MY, Chan JGY, and Chan H-K. Pulmonary drug delivery by powder aerosols. *J*
11
12 755 *Control Release*. 2014;193:228-240.
13
14 756 **57.** Chow AL, Tong HY, Chattopadhyay P, and Shekunov B. Particle Engineering for
15
16 757 Pulmonary Drug Delivery. *Pharm Res*. 2007;24:411-437.
17
18 758 **58.** Liang Z, Ni R, Zhou J, and Mao S. Recent advances in controlled pulmonary drug
19
20 759 delivery. *Drug Discov To*. 2015;20:380-389.
21
22
23 760 **59.** Heyder J, Gebhart J, Rudolf G, Schiller CF, and Stahlhofen W. Deposition of particles
24
25 761 in the human respiratory tract in the size range 0.005–15 μm . *J Aerosol Sci*.
26
27 762 1986;17:811-825.
28
29 763 **60.** Raula J, Seppälä J, Malm J, Karppinen M, Kauppinen EI. Structure and dissolution of
30
31 764 L-leucine-coated salbutamol sulphate aerosol particles. *AAPS PharmSciTech*. 2012;
32
33 765 13:707-12.
34
35 766 **61.** May S, Jensen B, Wolkenhauer M, Schneider M, Lehr CM. Dissolution techniques for
36
37 767 in vitro testing of dry powders for inhalation. *Pharm Res*. 2012;29:2157-66.
38
39 768 **62.** Knieke C, Azad MA, To D, Bilgili E, Davé RN. Sub-100 micron fast dissolving
40
41 769 nanocomposite drug powders. *Powder Technol*. 2015;271:49–60.
42
43
44 770 **63.** Patel B, Gupta N, and Ahsan F. Particle engineering to enhance or lessen particle
45
46 771 uptake by alveolar macrophages and to influence the therapeutic outcome. *Eur J*
47
48 772 *Pharm Biopharm*. 2015;89:163-174.
49
50 773 **64.** Kou X, Chan LW, Steckel H, and Heng PWS. Physico-chemical aspects of lactose for
51
52 774 inhalation. *Adv Drug Deliv Rev*. 2012;64:220-232.
53
54
55 775 **65.** Pilcer G, Wauthoz N, and Amighi K. Lactose characteristics and the generation of the
56
57 776 aerosol. *Adv Drug Deliv Rev*. 2012;64:233-256.
58
59
60

- 1
2
3 777 66. Prota L, Santoro A, Bifulco M, Aquino RP, Mencherini T, and Russo P. Leucine
4
5 778 enhances aerosol performance of Naringin dry powder and its activity on cystic
6
7 779 fibrosis airway epithelial cells. *Int J Pharm.* 2011;412:8-19.
8
9
10 780 67. Taki M, Marriott C, Zeng X-M, and Martin GP. Aerodynamic deposition of
11
12 781 combination dry powder inhaler formulations in vitro: A comparison of three
13
14 782 impactors. *Int J Pharm.* 2010;388:40-51.
15
16 783 68. Davis SS. Delivery of peptide and non-peptide drugs through the respiratory tract.
17
18 784 *Pharm Sci Techn To.* 1999;2:450-456.
19
20 785 69. Musante CJ, Schroeter JD, Rosati JA, Crowder TM, Hickey AJ, and Martonen TB.
21
22 786 Factors affecting the deposition of inhaled porous drug particles. *J Pharm Sci.*
23
24 787 2002;91:1590-1600.
25
26 788 70. Lechuga-Ballesteros D, Charan C, Stults CL, Stevenson CL, Miller DP, Vehring R,
27
28 789 Tep V, and Kuo MC. Trileucine improves aerosol performance and stability of spray-
29
30 790 dried powders for inhalation. *J Pharm Sci.* 2008;97:287-302.
31
32 791 71. Chew NY and Chan HK. The role of particle properties in pharmaceutical powder
33
34 792 inhalation formulations. *J Aerosol Med.* 2002;15:325-330.
35
36 793 72. Brand-Williams W, Cuvelier ME, and Berset C. Use of a free radical method to
37
38 794 evaluate antioxidant activity. *LWT - Food Science and Technology.* 1995;28:25-30.
39
40 795 73. Villaño D, Fernández-Pachón MS, Moyá ML, Troncoso AM, and García-Parrilla MC.
41
42 796 Radical scavenging ability of polyphenolic compounds towards DPPH[•] free radical.
43
44 797 *Talanta.* 2007;71:230-235.
45
46 798 74. Al Shaal L, Shegokar R, and Muller RH. Production and characterization of
47
48 799 antioxidant apigenin nanocrystals as a novel UV skin protective formulation. *Int J*
49
50 800 *Pharm.* 2011;420:133-140.
51
52
53
54
55
56
57
58
59
60

- 1
2
3 801 75. Papay Z.E AI. Study on the antioxidant activity during the formulation of biological
4
5 802 active ingredient. *European Scientific Journal*. 2014;Special Edition 3:252-257.
6
7 803 76. Yang J, Guo J, and Yuan J. In vitro antioxidant properties of rutin. *LWT - Food*
8
9 804 *Science and Technology*. 2008;41:1060-1066.
10
11 805 77. Natella F, Nardini M, Di Felice M, and Scaccini C. Benzoic and Cinnamic Acid
12
13 806 Derivatives as Antioxidants: Structure–Activity Relation. *J Agr Food Chem*.
14
15 807 1999;47:1453-1459.
16
17
18 808 78. Roche M, Rondeau P, Singh NR, Tarnus E, and Bourdon E. The antioxidant properties
19
20 809 of serum albumin. *FEBS Lett*. 2008;582:1783-1787.
21
22
23 810 79. Fang R, Jing H, Chai Z, Zhao G, Stoll S, Ren F, Liu F, and Leng X. Study of the
24
25 811 physicochemical properties of the BSA: flavonoid nanoparticle. *Eur Food Res*
26
27 812 *Technol*. 2011;233:275-283.
28
29
30 813
31
32 814
33
34
35
36
37
38
39
40
41
42
43
44
45
46
47
48
49
50
51
52
53
54
55
56
57
58
59
60

815 TABLES

816 Table 1

817 Aerosol particle sizes of spray-dried nanoparticles with Sympatec HELOS laser
818 diffractometer in μm .

	Excipient-free	Lactose	L-leucine
ED (%)	91.862 ± 2.735	93.950 ± 1.046	95.183 ± 0.667
FPF (%)	65.617 ± 3.422	58.463 ± 6.031	66.090 ± 2.777
MMAD (μm)	3.210 ± 0.069	3.130 ± 0.001	2.123 ± 0.098
GSD (μm)	2.823 ± 0.113	2.270 ± 0.212	1.887 ± 0.063
RD (%)	99.1 ± 5.012	94.7 ± 4.091	96.3 ± 2.161

819

820

821 Table 2

822 Aerodynamic characteristic of spray-dried nanoparticles.

	Excipient-free	Lactose	L-leucine
D ₁₀	1.033 ± 0.032	1.020 ± 0.070	0.843 ± 0.680
D ₅₀	3.030 ± 0.092	3.107 ± 0.102	2.473 ± 0.300
D ₉₀	7.110 ± 0.306	7.117 ± 0.337	5.287 ± 0.670

823

824

825 **FIGURE CAPTIONS**

826 **Figure 1.** Molecular structure of apigenin.

827 **Figure 2.** Fluorescence emission spectra of BSA solution, BSA nanoparticles and BSA-Api
828 nanoparticles. The excitation wavelength was set to 285 nm (EM: emission, EXC:
829 excitation)

830 **Figure 3.** Three dimensional fluorescence emission maps and two dimensional contour
831 maps of empty BSA nanoparticles and BSA-Api nanoparticles. Color scale
832 displays the range of observed fluorescence intensities.

833 **Figure 4. A)** FT-IR spectra of apigenin (1), BSA (2) and the excipient-free spray-dried
834 BSA-Api nanoparticles (3).

835 **B)** FT-IR spectra of apigenin (1), BSA (2), lactose (3) and the spray-dried BSA-
836 Api nanoparticles with lactose (4).

837 **C)** FT-IR spectra of apigenin (1), BSA (2), L-leucine (3) and the spray-dried
838 BSA-Api nanoparticles with L-leucine (4).

839 **Figure 5.** XRPD diffraction pattern of raw apigenin and the formulations.

840 **Figure 6. A)** DSC thermograms of apigenin (1), BSA (2) physical mixture (3) and the
841 excipient-free spray dried BSA-Api nanoparticles (4).

842 **B)** DSC spectra of apigenin (1), BSA (2), physical mixture (3) and the spray-dried
843 BSA-Api nanoparticles with lactose (4).

844 **C)** DSC spectra of apigenin (1), BSA (2), physical mixture (3) and the spray-dried
845 BSA-Api nanoparticles with L-leucine (4).

846 **Figure 7. A)** Solubility of spray dried BSA-Api formulations in PBS buffer and modified
847 simulated lung fluid (mSLF).

848 **B)** Dissolution of apigenin from the formulations as a function of time in modified
849 simulated lung fluid (mSLF).

1
2
3 850 **Figure 8.** NGI deposition pattern of the spray dried BSA-API formulations.

4 851 **Figure 9.** SEM images of raw apigenin (1), excipient-free spray dried BSA-API
5
6 852 nanoparticles (2), spray-dried BSA-API nanoparticles with lactose (3), spray-dried
7
8 853 BSA-API nanoparticles with L-leucine (4) 20000 x magnification.

9
10
11 854 **Figure 10.** Radical scavenging activity of Apigenin solution, empty BSA nanoparticles,
12
13 855 BSA-Apigenin nanoparticles (NP) and spray-dried nanoparticles (SD) with
14
15 856 excipients. The antioxidant activity is expressed as the inhibition of DPPH[•] free
16
17 857 radical in percent.

18
19
20 858 **To whom correspondence should be addressed:**

21
22 859 antal.istvan@pharma.semmelweis-univ.hu

23
24 860 Department of Pharmaceutics

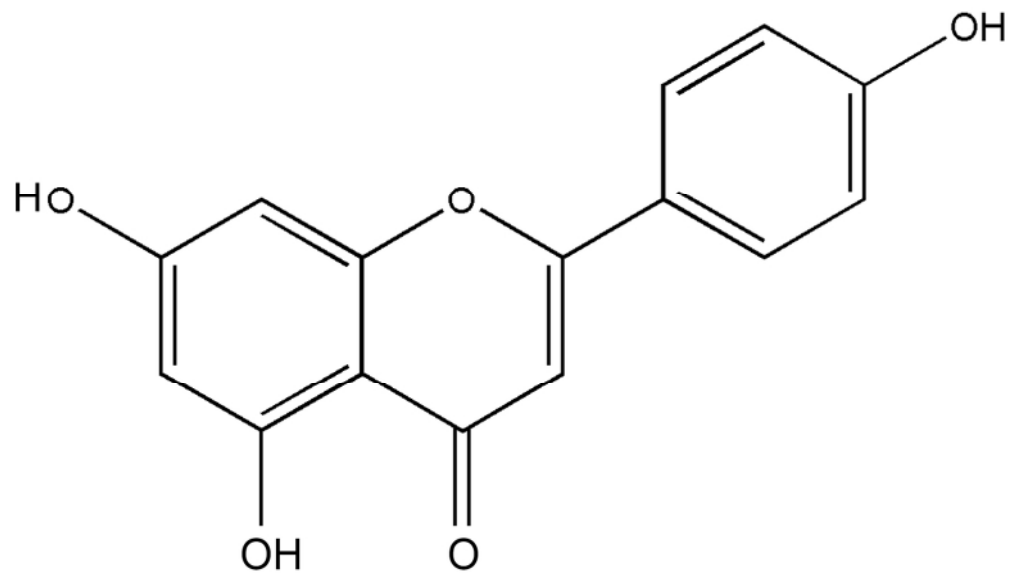
25
26 861 Semmelweis University

27
28 862 Hőgyes E. Street 7-9,

29
30 863 H-1092 Budapest, Hungary

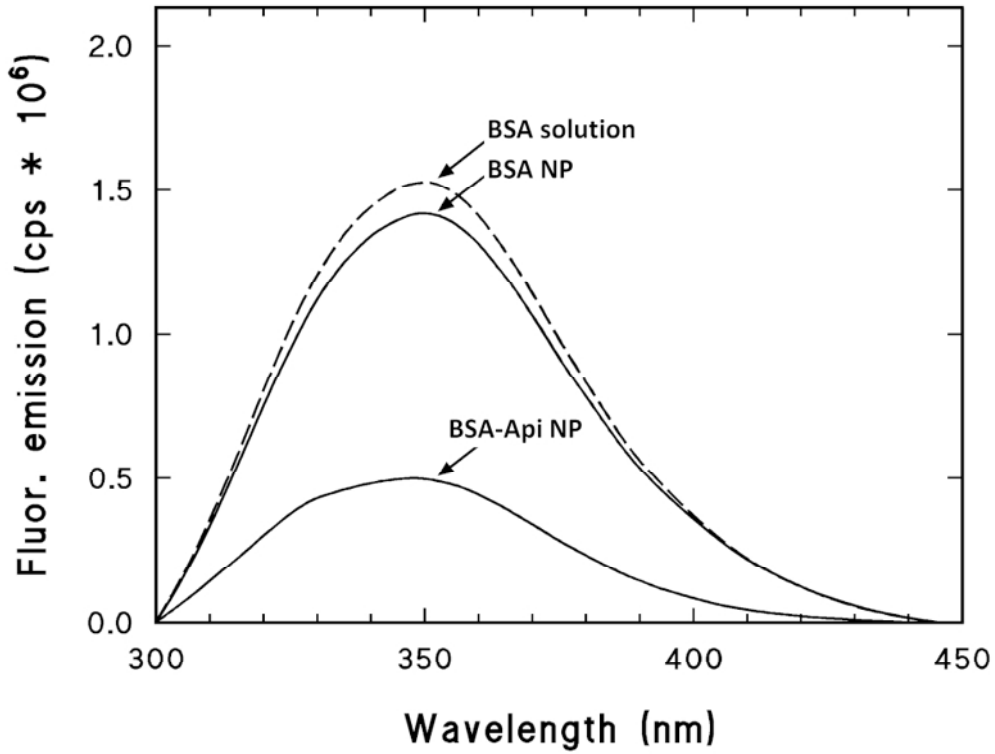
31
32 864 Tel/Fax: +3612017-0914; Tel.: +361476-3600/53066, 53087

33
34
35 865
36
37
38
39
40
41
42
43
44
45
46
47
48
49
50
51
52
53
54
55
56
57
58
59
60



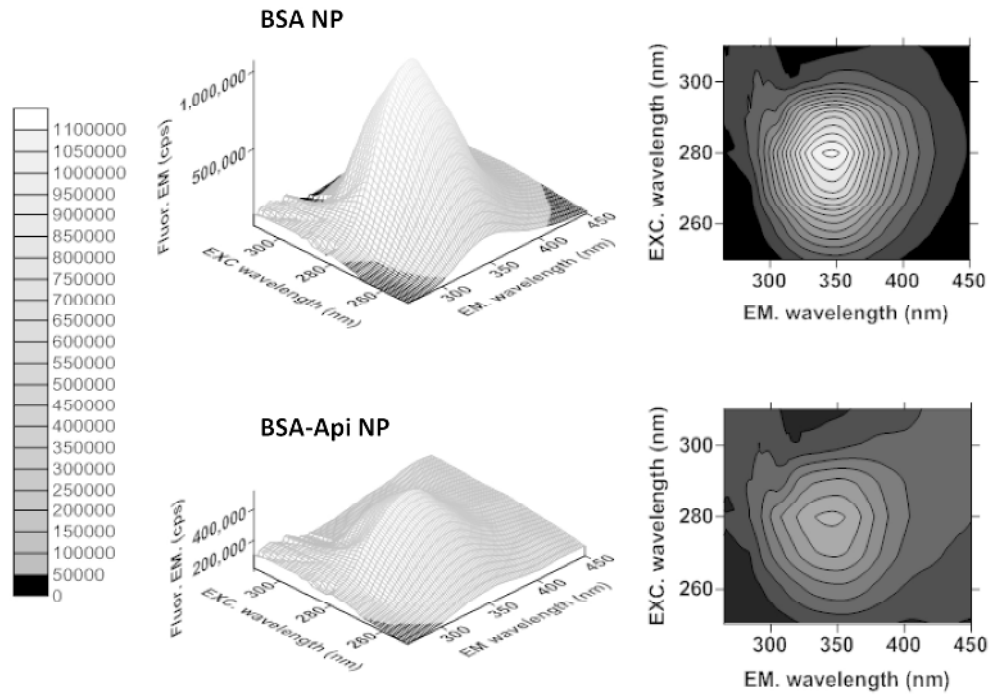
Molecular structure of apigenin.

45x25mm (600 x 600 DPI)



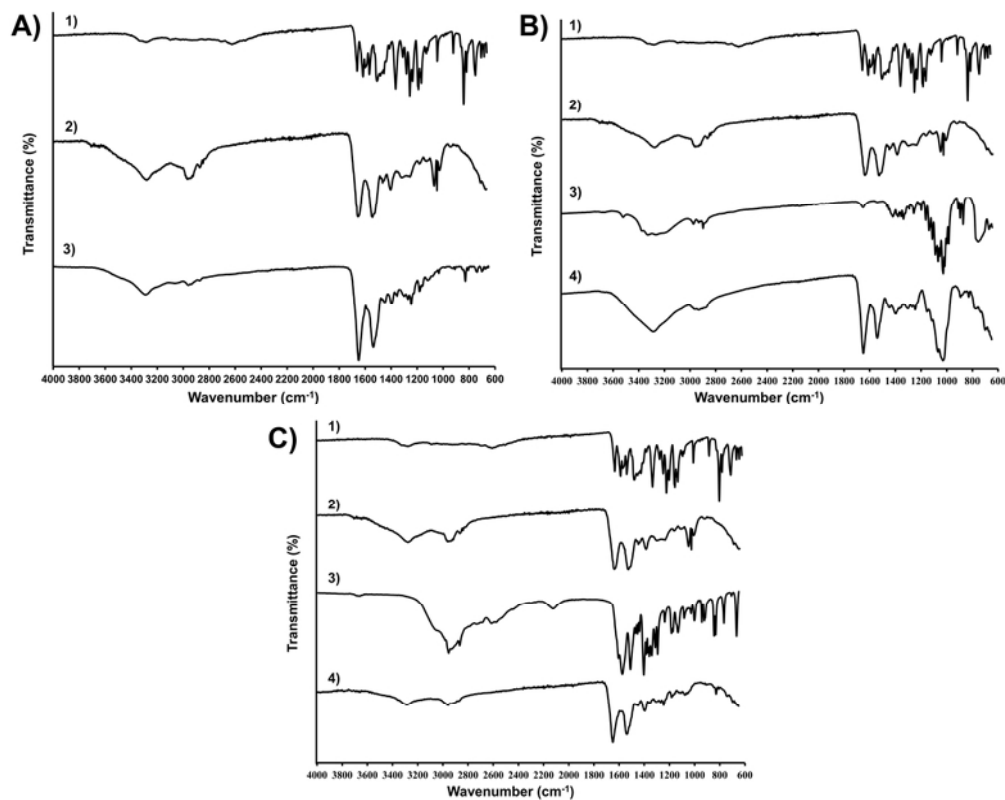
Fluorescence emission spectra of BSA solution, BSA nanoparticles and BSA-Api nanoparticles. The excitation wavelength was set to 285 nm (EM: emission, EXC: excitation)

80x60mm (300 x 300 DPI)



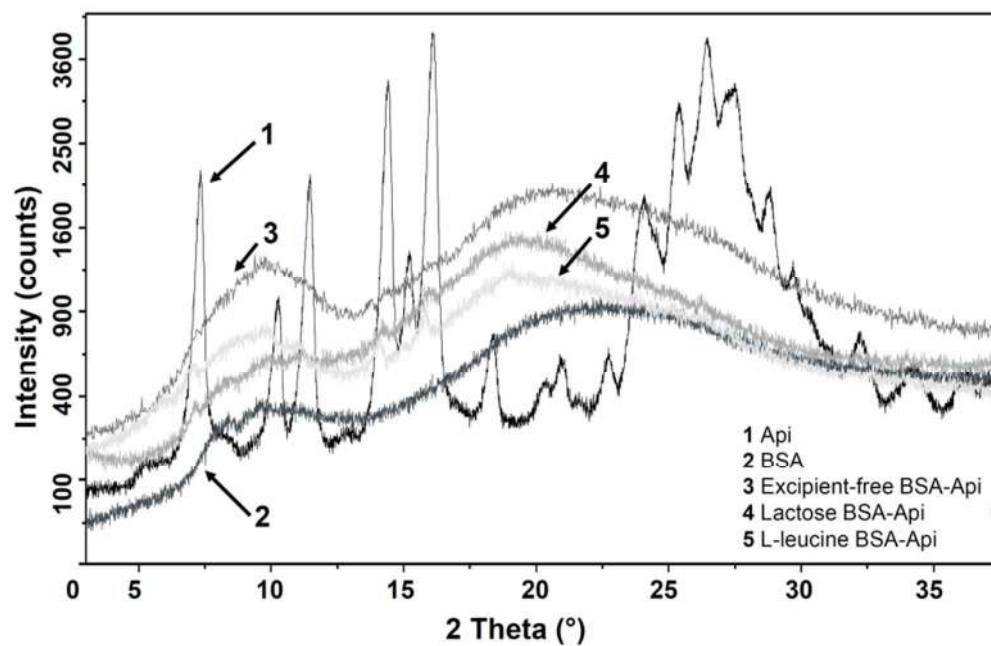
Three dimensional fluorescence emission maps and two dimensional contour maps of empty BSA nanoparticles and BSA-Api nanoparticles. Color scale displays the range of observed fluorescence intensities.

160x110mm (300 x 300 DPI)



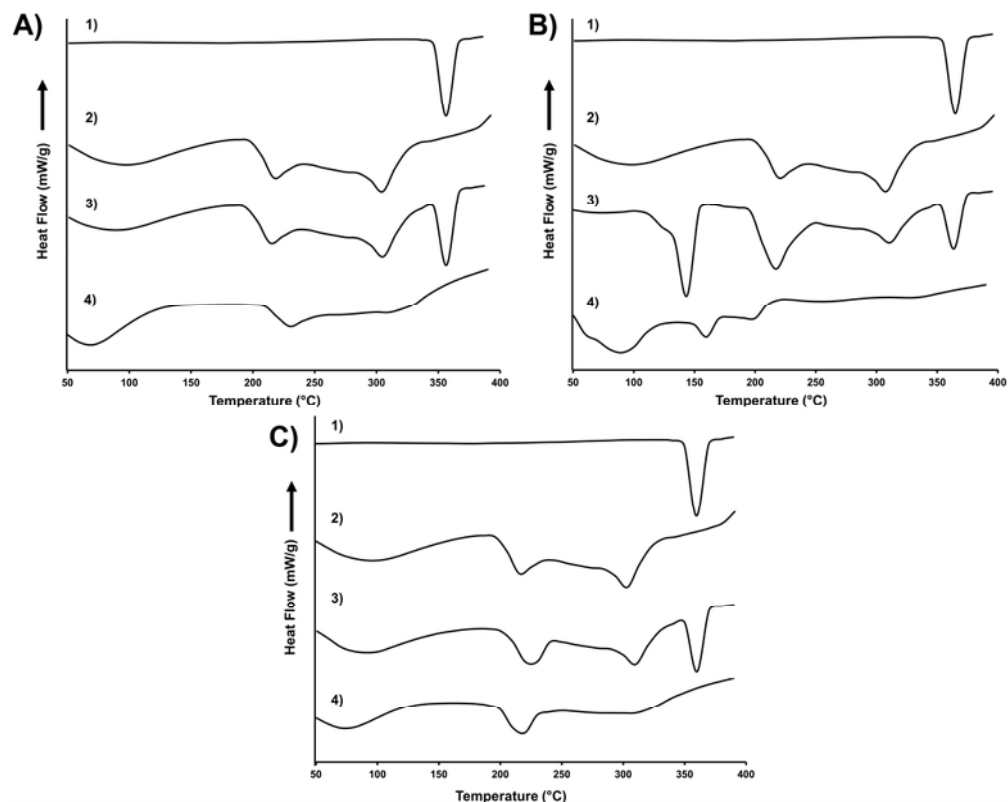
- A) FT-IR spectra of apigenin (1), BSA (2) and the excipient-free spray-dried BSA-Api nanoparticles (3).
B) FT-IR spectra of apigenin (1), BSA (2), Lactohale® (3) and the spray-dried BSA-Api nanoparticles with Lactohale® (4).
C) FT-IR spectra of apigenin (1), BSA (2), L-leucine (3) and the spray-dried BSA-Api nanoparticles with L-leucine (4).

42x34mm (600 x 600 DPI)



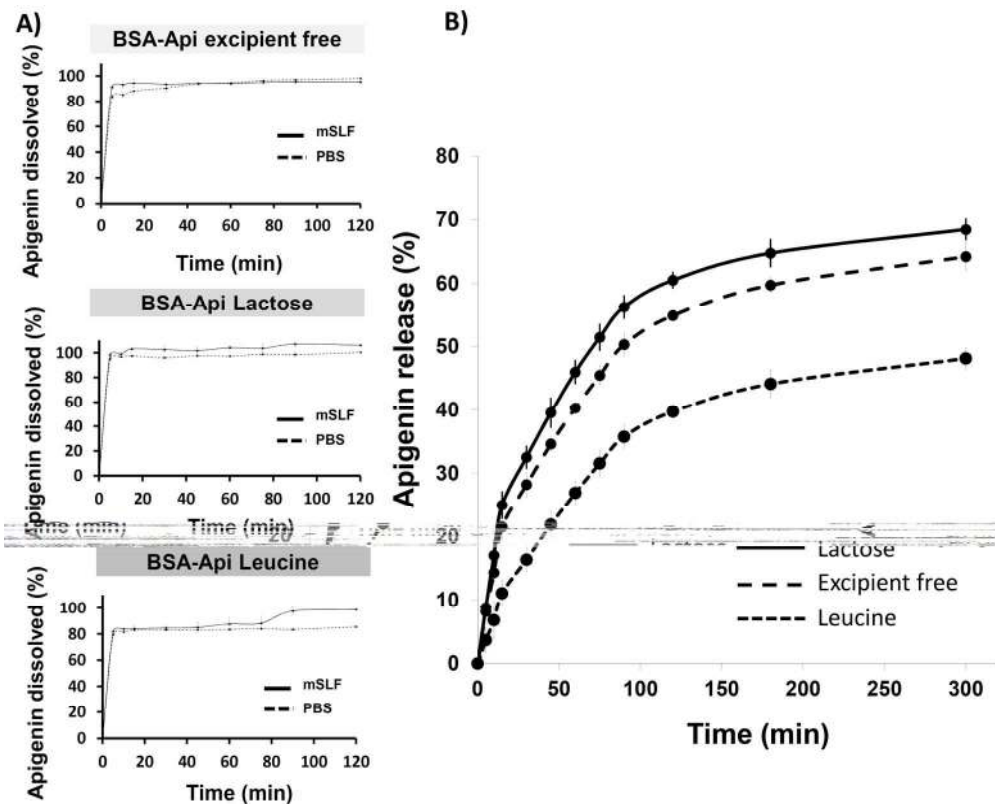
XRPD diffraction pattern of raw apigenin and the formulations.

80x52mm (300 x 300 DPI)



- A) DSC thermograms of apigenin (1), BSA (2) physical mixture (3) and the excipient-free spray dried BSA-Api nanoparticles (4).
- B) DSC spectra of apigenin (1), BSA (2), physical mixture (3) and the spray-dried BSA-Api nanoparticles with Lactohale® (4).
- C) DSC spectra of apigenin (1), BSA (2), physical mixture (3) and the spray-dried BSA-Api nanoparticles with L-leucine (4).

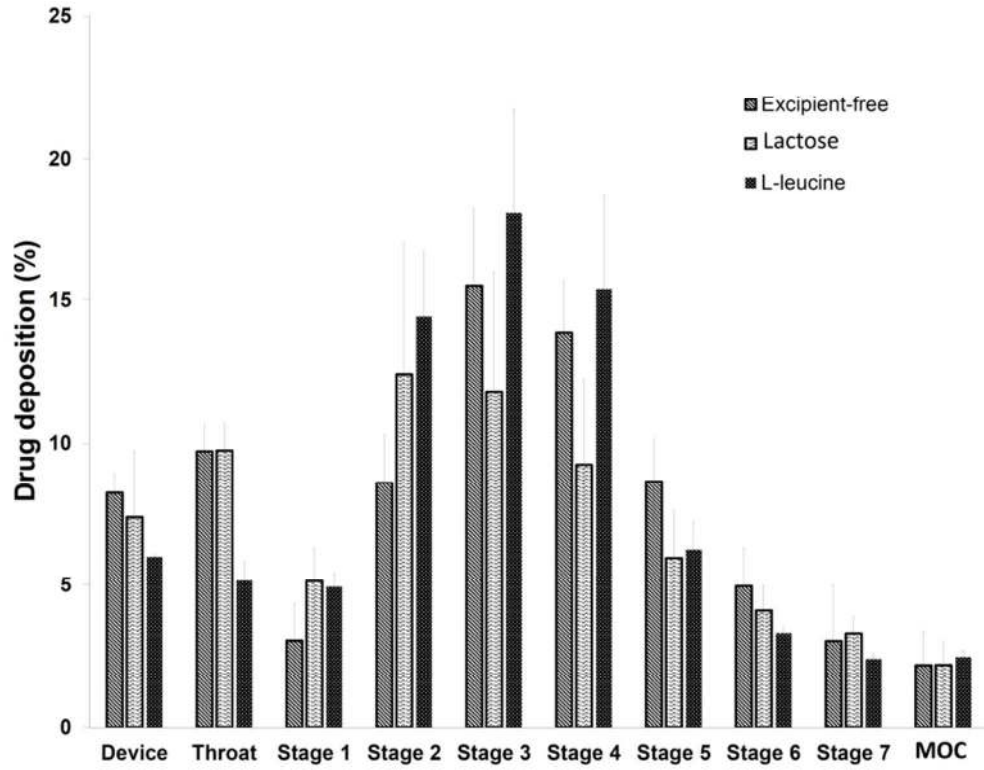
42x34mm (600 x 600 DPI)



A) Solubility of spray dried BSA-Api formulations in PBS buffer and modified simulated lung fluid (mSLF).

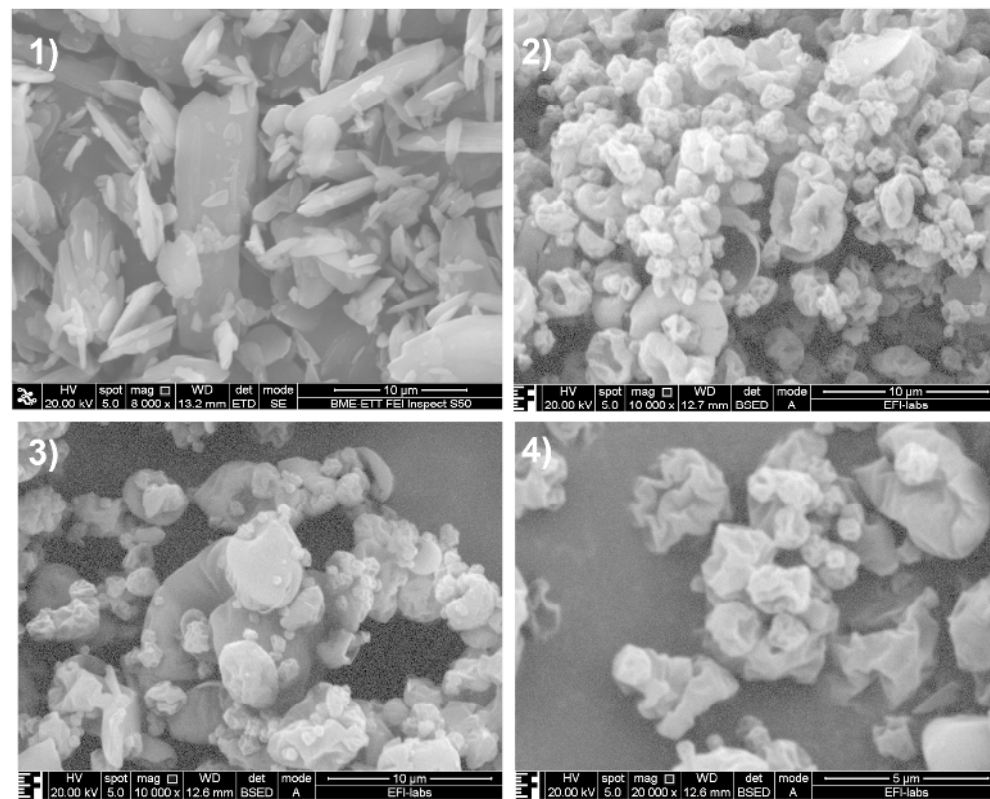
B) Dissolution of apigenin from the formulations as a function of time in modified simulated lung fluid (mSLF).

160x128mm (300 x 300 DPI)



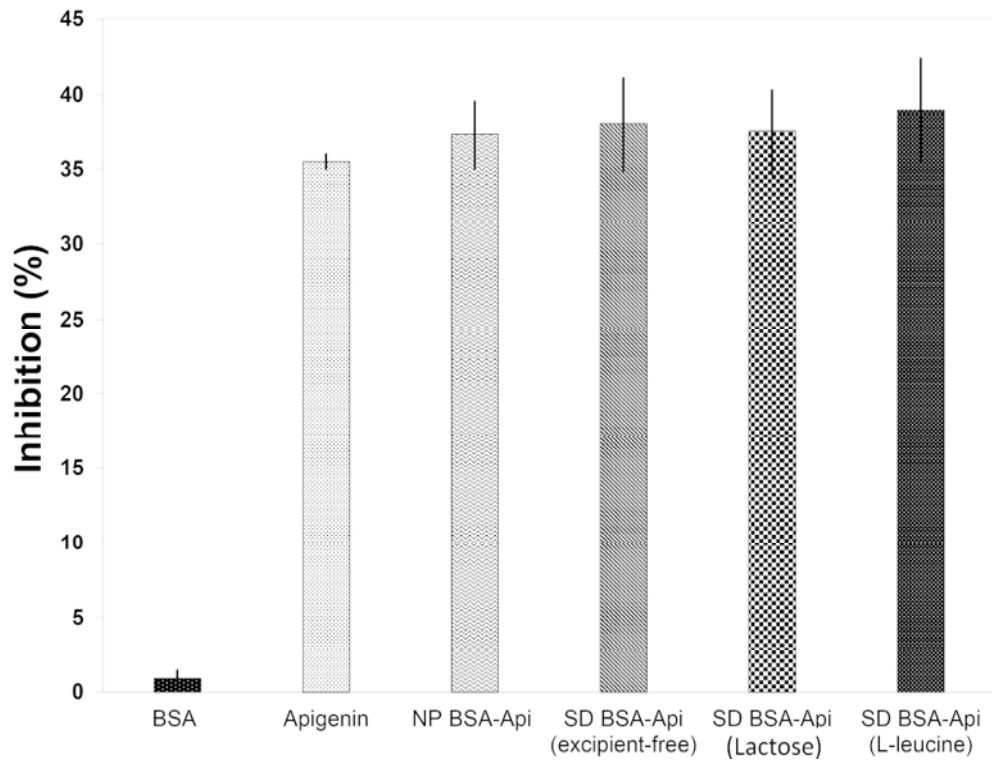
NGI deposition pattern of the spray dried BSA-API formulations.

80x61mm (300 x 300 DPI)



SEM images of raw apigenin (1), excipient-free spray dried BSA-Api nanoparticles (2), spray-dried BSA-Api nanoparticles with lactose (3), spray-dried BSA-Api nanoparticles with L-leucine (4) 20000 x magnification.

160x127mm (300 x 300 DPI)



Radical scavenging activity of Apigenin solution, empty BSA nanoparticles, BSA-Apigenin nanoparticles (NP) and spray-dried nanoparticles (SD) with excipients. The antioxidant activity is expressed as the inhibition of DPPH[•] free radical in percent.

80x60mm (300 x 300 DPI)